

Synergistic cooperation and crosstalk between *MYD88*^{L265P} and mutations that dysregulate CD79B and surface IgM

James Q. Wang,¹ Yogesh S. Jeelall,¹ Peter Humburg,² Emma L. Batchelor,¹ Sarp M. Kaya,¹ Hee Min Yoo,³ Christopher C. Goodnow,^{2*} and Keisuke Horikawa^{1*}

¹Australian Cancer Research Foundation Department of Cancer Biology and Therapeutics, The John Curtin School of Medical Research, The Australian National University, Canberra, Australia

²Garvan Institute of Medical Research, Sydney, Australia

³Lymphoid Malignancies Branch, Center for Cancer Research, National Cancer Institute, National Institutes of Health, Bethesda, MD

CD79B and *MYD88* mutations are frequently and simultaneously detected in B cell malignancies. It is not known if these mutations cooperate or how crosstalk occurs. Here we analyze the consequences of *CD79B* and *MYD88*^{L265P} mutations individually and combined in normal activated mouse B lymphocytes. *CD79B* mutations alone increased surface IgM but did not enhance B cell survival, proliferation, or altered NF- κ B responsive markers. Conversely, B cells expressing *MYD88*^{L265P} decreased surface IgM coupled with accumulation of endoglycosidase H-sensitive IgM intracellularly, resembling the trafficking block in anergic B cells repeatedly stimulated by self-antigen. Mutation or overexpression of *CD79B* counteracted the effect of *MYD88*^{L265P}. In B cells chronically stimulated by self-antigen, *CD79B* and *MYD88*^{L265P} mutations in combination, but not individually, blocked peripheral deletion and triggered differentiation into autoantibody secreting plasmablasts. These results reveal that *CD79B* and surface IgM constitute a rate-limiting checkpoint against B cell dysregulation by *MYD88*^{L265P} and provide an explanation for the co-occurrence of *MYD88* and *CD79B* mutations in lymphomas.

INTRODUCTION

Diffuse large B cell lymphoma (DLBCL) is one of the most frequent and aggressive B cell malignancies (Lenz and Staudt, 2010). The activated B cell type of DLBCL (ABC-DLBCL) represents a particularly aggressive form, distinguished by constitutive activation of the canonical NF- κ B transcription factor family and by poor patient survival and response to the standard treatment regimen of R-CHOP (Lenz and Staudt, 2010). NF- κ B transcription factors are normally activated by two key receptors for microbes on B cells, the B cell antigen receptor (BCR) and the TLRs, and serve as essential inducers of normal B cell survival, growth, and differentiation (Thome, 2004; Gerondakis and Siebenlist, 2010; Hayden and Ghosh, 2012). Somatic mutations in *CD79B* and *MYD88*, affecting critical proteins for BCR and TLR signaling, respectively, are recurrently found together in ABC-DLBCLs (Lenz et al., 2008; Davis et al., 2010; Ngo et al., 2011). It is not known if these mutations act cooperatively to dysregulate B

cell survival, growth, or other functions or how cooperation and crosstalk might occur.

Missense mutations in *MYD88* occur in 39% of cases of ABC-DLBCLs, with a single L265P amino acid substitution accounting for 75% of the mutations (Ngo et al., 2011). The same *MYD88*^{L265P} mutation occurs in almost 100% of Waldenström macroglobulinemia (WM), 47% of IgM monoclonal gammopathy of undetermined significance, and 3–10% of chronic lymphocytic leukemia (Puente et al., 2011; Wang et al., 2011; Treon et al., 2012; Xu et al., 2013). *MYD88* is an essential cytoplasmic adaptor protein, downstream from most TLRs and the IL-1/18 receptor, required to activate the IL-1 receptor-associated kinases (IRAKs) and NF- κ B (Akira and Takeda, 2004). *MYD88* has two distinct domains. A Toll/IL-1R domain (TIR) promotes homotypic and heterotypic multimerization of *MYD88* proteins upon recruitment to dimerized TIR domains in the cytoplasmic tail of TLRs that have been engaged by their microbial ligands (Vyncke et al., 2016). A death domain forms a helical multimeric signaling complex known as the Myddosome comprising six *MYD88* molecules, four IRAK4 molecules, and four IRAK2 molecules (Akira and Takeda, 2004; Lin et al., 2010). The *MYD88*^{L265P} mutation in the TIR domain is predicted to cause allosteric changes in two binding surfaces and has been shown to promote multimerization with wild-type *MYD88*

*C.C. Goodnow and K. Horikawa contributed equally to this paper.

Correspondence to Christopher C. Goodnow: c.goodnow@garvan.org.au; Keisuke Horikawa: keisuke.horikawa@anu.edu.au

J.Q. Wang's present address is Lymphoid Malignancies Branch, Center for Cancer Research, National Cancer Institute, National Institutes of Health, Bethesda, MD.

Abbreviations used: ABC, activated B cell like; BCR, B cell receptor; BTK, Bruton tyrosine kinase; DLBCL, diffuse large B cell lymphoma; Endo H, endoglycosidase H; ERK, extracellular signal-related kinase; FDR, false discovery rate; HEL, hen egg lysozyme; IKK, I κ B kinase β ; IRAK, IL-1 receptor-associated kinase; ITAM, immunoreceptor tyrosine-based activation motif; PI3K, phosphoinositide 3-kinase; TIR, Toll/IL-1R domain; WM, Waldenström macroglobulinemia.

© 2017 Wang et al. This article is distributed under the terms of an Attribution-Noncommercial-Share Alike-No Mirror Sites license for the first six months after the publication date (see <http://www.rupress.org/terms/>). After six months it is available under a Creative Commons License (Attribution-Noncommercial-Share Alike 4.0 International license, as described at <https://creativecommons.org/licenses/by-nc-sa/4.0/>).



and spontaneous formation of the MYD88-IRAK signaling complex, resulting in elevated NF- κ B activity (Ngo et al., 2011; Avbelj et al., 2014; Vyncke et al., 2016). When introduced into mature mouse B cells by retroviral transduction, *MYD88^{L265P}* is sufficient to initiate mitogen and T cell independent B cell proliferation that is terminated after several cell divisions, in part by feedback inhibition of NF- κ B (Wang et al., 2014). More recently, a mouse model bearing a conditional *Myd88^{L252P}* allele has been described to develop lymphoproliferative disease with occasional transformation into clonal lymphomas (Knittel et al., 2016). Conversely, knockdown of MYD88 potently kills ABC-DLBCL cell lines, establishing that these tumors are addicted to MYD88 activation for survival (Ngo et al., 2011).

Somatic mutations in *CD79B* occur in 21% of ABC-DLBCLs (Davis et al., 2010). *CD79B* and *CD79A* associate noncovalently with membrane immunoglobulin, serving as the signal-transducing subunits of the BCR through an immunoreceptor tyrosine-based activation motif (ITAM) in the *CD79B* and *CD79A* cytoplasmic tails (Reth and Wienands, 1997). Upon antigen binding, the two tyrosines in each ITAM are phosphorylated by LYN and other SRC-family kinases, providing a docking site for the paired SH2 domains of SYK, activating SYK, and initiating the intracellular signaling cascade (Cambier et al., 1994). 85% of *CD79B* mutations substitute the first ITAM tyrosine residue at position 196 (Y196) to another amino acid, most frequently histidine (Davis et al., 2010). Unlike *MYD88* mutations, *CD79B* ITAM mutations do not spontaneously activate NF- κ B in ABC-DLBCL cell lines (Lenz et al., 2008; Davis et al., 2010). Instead, *CD79B* ITAM mutations cause elevated surface BCR expression, possibly by inhibiting Lyn-mediated receptor internalization, resulting in higher surface BCR expression on ABC-DLBCLs but not in other tumors absent for *CD79B* mutations (Davis et al., 2010). In mice with a targeted mutation substituting alanine in place of both tyrosine residues in the *CD79B* ITAM, the mature B cells displayed more BCRs on their surface, had delayed BCR internalization after antigen binding, and had exaggerated BCR signaling to calcium, extracellular signal-regulated kinase (ERK), and AKT but normal signaling to NF- κ B (Gazumyan et al., 2006). Therefore, it is speculated that the likely role of *CD79B* mutation in the pathogenesis of ABC-DLBCL is by allowing B cells to respond inappropriately to BCR stimulation by foreign or self-antigens (Rui et al., 2011). However this hypothesis remains to be tested experimentally.

One third of ABC-DLBCLs bearing the *MYD88^{L265P}* mutation also have *CD79B* ITAM mutations (Ngo et al., 2011). shRNA knockdown of *CD79B* and other components in BCR signaling in ABC-DLBCLs synergizes with shRNA against *MYD88* in killing ABC-DLBCL cell lines in vitro, suggesting that BCR signaling through *CD79B* plays an important and nonredundant role in supplementing the growth and survival of *MYD88^{L265P}* tumors (Ngo et al., 2011). In a phase 1/2 clinical trial of the Bruton tyrosine kinase (BTK)

inhibitor ibrutinib, complete or partial responses occurred in four of five patients with ABC-DLBCL bearing both *CD79B* and *MYD88^{L265P}* mutations, contrasting with zero of seven patients with *MYD88^{L265P}* ABC-DLBCL without *CD79B* mutations (Wilson et al., 2015). However, it is not known if *CD79B* and *MYD88* mutations cooperate to dysregulate normal B cell survival and growth or how such cooperation might impose dependency on BTK. Addressing this question may also illuminate fundamental mechanisms of synergistic and antagonistic crosstalk between antigen receptor and TLR signals in B cells (Rui et al., 2003, 2006).

B cells actively acquire tolerance to self-antigens through a series of bone marrow and peripheral lymphoid tissue checkpoints that inhibit B cell survival, growth, and plasma cell differentiation (Goodnow, 2007). B cells undergo multiple rounds of clonal proliferation upon binding to foreign antigen, but undergo anergy or apoptosis when their receptors are repeatedly engaged by self-antigens. Many human DLBCLs, and to a lesser extent follicular, marginal zone, and Burkitt's lymphoma cells, express BCRs that are self-reactive because they use the VH4-34 element (Silberstein et al., 1991; Zhu et al., 1994; Hsu and Levy, 1995; Ottensmeier et al., 1998; Lossos et al., 2000; Young et al., 2015), which binds to human erythrocyte I-i polysaccharide antigen and human B lymphocyte CD45 O-linked polysaccharide antigen (Pascual et al., 1991; Grillot-Courvalin et al., 1992). A recent study showed that self-antigen engagement of the BCR is required for the survival of some ABC-DLBCL cells, notably in a VH4-34⁺ lymphoma in which point mutations in the binding site that disrupt self I-i binding diminished the capacity of that BCR to support survival or growth of the lymphoma in tissue culture (Young et al., 2015). In healthy people, VH4-34⁺ B cells with intact I-i binding sites are negatively selected against accumulating in the germinal center, memory B cell, or plasma cell repertoires (Pugh-Bernard et al., 2001; Reed et al., 2016). Therefore, a key question is whether *CD79B* mutations disrupt normal peripheral B cell tolerance checkpoints and switch the B cell response to self-antigen from apoptosis into proliferation, as has been shown for *CARD11* mutations (Jeelall et al., 2012).

Here, we analyze the consequences of *CD79B* mutations in normal B cells and test if cooperation between *MYD88* and *CD79B* somatic mutations disrupts peripheral self-tolerance checkpoints in B cells. We show that *CD79B* mutation on its own does not promote spontaneous growth or survival, nor does it block self-antigen-induced peripheral tolerance. However, extraordinary epistasis between *CD79B* and *MYD88^{L265P}* occurs when coexpressed, blocking self-tolerance checkpoints and promoting spontaneous plasmablast differentiation. We show that *MYD88^{L265P}* spontaneously triggers a block in intracellular processing and surface expression of BCRs similar to that observed in self-reactive B cells, and this block is relieved either by *CD79B* ITAM mutation or by increasing expression of wild-type *CD79B*. These findings reveal an unexpected, po-

tent crosstalk and cooperation between mutations affecting the BCR and TLR signaling pathways and provide an explanation for the frequent co-occurrence of *MYD88* and *CD79B* mutations in ABC-DLBCLs.

RESULTS

CD79B ITAM mutations do not drive B cell proliferation or NF- κ B response genes

To model the acquisition by activated B cells of somatic mutations in *MYD88* and *CD79B*, we transiently activated normal spleen B cells with a 6-h exposure to hen egg lysozyme (HEL) antigen in vivo followed by 24-h culture with anti-CD40 antibody but no further exposure to BCR ligand. The activated B cells were then transduced with retroviral vectors during a further 36-h culture with anti-CD40 antibody but not BCR ligand, after which the cells were washed free of anti-CD40 and cultured in medium alone. When activated B cells are transduced with vectors encoding *MYD88^{L265P}* or *CARD11^{L232LI}* and then placed back into culture with no mitogen, they are induced to divide repeatedly, in contrast to control cells transduced with empty vector or vectors encoding normal versions of these proteins, which do not divide but instead rapidly die (Jeelall et al., 2012; Wang et al., 2014). We therefore used the same assay to test if retroviral expression of *CD79B* bearing ITAM mutations found in lymphomas could also drive mitogen-independent cell proliferation in otherwise normal B cells. We transduced activated mature B cells with bicistronic EGFP vectors encoding either wild-type *CD79B* or *CD79B* with missense mutations in the first ITAM tyrosine, corresponding to the recurring human Y196H or Y196F mutations (Davis et al., 2010), or a Y207F substitution in the second ITAM, or Y196F combined with Y207F (Fig. 1, A and B). After transduction, the cells were washed and placed back in culture for 3 d. In the absence of mitogen, the numbers of live EGFP⁺ B cells steadily declined at the same rate as empty vector transduced B cells that expressed only EGFP, and at the same rate as EGFP⁻ cells in the same culture (Fig. 1 B). Thus, enforced expression of *CD79B* wild-type or mutants alone conferred no measurable survival advantage to primary B cells. Analysis of cell trace violet dilution also showed no induction of cell division (not depicted).

The cell surface proteins CD23 and CD25 are encoded by genes directly induced by NF- κ B, and both are markedly increased on primary B cells transduced with retroviral vectors encoding mutant alleles of *CARD11* or I κ B kinase β (IKK) found in human lymphomas (Wang et al., 2014). Using the same assay, expression of *CD79B* ITAM mutant proteins did not induce surface CD23 on EGFP⁺ cells relative to nontransduced EGFP⁻ cells in the same culture, relative to EGFP⁺ cells expressing wild-type *CD79B* or empty vector (Fig. 1 C). Nor did the expression of *CD79B* ITAM mutant proteins induce surface CD25 relative to EGFP⁺ cells expressing wild-type *CD79B* (Fig. 1 C).

Because Y196H is the most frequent *CD79B* mutation co-occurring with *MYD88^{L265P}* (Davis et al., 2010), we next

analyzed the consequences of *CD79B^{Y196H}* coexpressed with *MYD88^{L265P}*. Coexpression of *CD79B^{Y196H}* and *MYD88^{L265P}* failed to extend the transient phase of B cell proliferation induced by *MYD88^{L265P}* alone in vitro (Fig. 1 D). The lack of any effect contrasts with the extended proliferation when *MYD88^{L265P}* was combined with loss-of-function mutations in *Tnfrsf10b* (A20) or *Bcl2l1* (BIM) or gain-of-expression of *Bcl2* (Wang et al., 2014). To assess whether *CD79B* mutation affected the negative feedback of NF- κ B by *MYD88^{L265P}*, we also measured NF- κ B-inducible protein markers on doubly transduced B cells as previously described (Wang et al., 2014). As a positive control, we also transduced B cells with IKK bearing an activating mutation found in human lymphoma, which strongly induced CD23, CD25, and CD95 (Jeelall et al., 2012). In contrast, all markers were down-regulated relative to empty vector controls on B cells expressing *MYD88^{L265P}* alone and were comparably down-regulated on B cells coexpressing *CD79B^{Y196H}* and *MYD88^{L265P}* (Fig. 1 E). The lack of any measurable effect of *CD79B* in these assays contrasts with our previous findings, in which loss-of-function mutations in *Tnfrsf10b* (A20) blocked *MYD88^{L265P}*-induced down-regulation of CD23, CD25, CD86, and CD95 (Wang et al., 2014).

CD79B and *MYD88* mutations have opposing and complementary effects on surface BCR expression

Next we considered whether *CD79B* ITAM mutations affected surface BCR expression on retrovirally transduced primary B cells, because lymphomas with *CD79B* mutations have elevated BCR expression (Davis et al., 2010). Activated mature B cells were transduced with retroviral vectors, cultured in the absence of mitogen for 24 h, and analyzed by flow cytometry for surface *CD79B* and IgM. Compared with B cells transduced with empty vector, B cells expressing the wild-type *CD79B* retroviral vector had 150% increased surface *CD79B* and surface IgM, while this was increased to 200% of empty vector controls in cells expressing *CD79B^{Y196H}* (Fig. 2 A). In contrast, surface *CD79B* and IgM were dramatically decreased on EGFP⁺ cells expressing *MYD88^{L265P}* alone, representing only 30% of the levels on empty vector EGFP⁺ cells (Fig. 2 B).

These convergent but opposing effects of mutant *MYD88* and *CD79B* on BCR surface levels were then analyzed in more detail. Surface IgM and *CD79B* were decreased by expression of the L265P mutant but not wild-type *MYD88* (Fig. 2 C). A cell surface protein not part of the BCR complex, CD44, was unaffected. Dual expression of *CD79B^{WT} MYD88^{L265P}* or *CD79B^{Y196H} MYD88^{L265P}* in B cells opposed the reduction of surface *CD79B* and IgM caused by *MYD88^{L265P}* alone, resulting in receptor levels comparable to empty vector controls but lower than cells with the *CD79B* vectors but without *MYD88^{L265P}* (Fig. 2 C).

These results revealed an unexpected inhibitory effect of *MYD88^{L265P}* on surface IgM receptor levels. To test if this occurred at the level of gene transcription, we measured mRNAs encoding the four protein subunits required

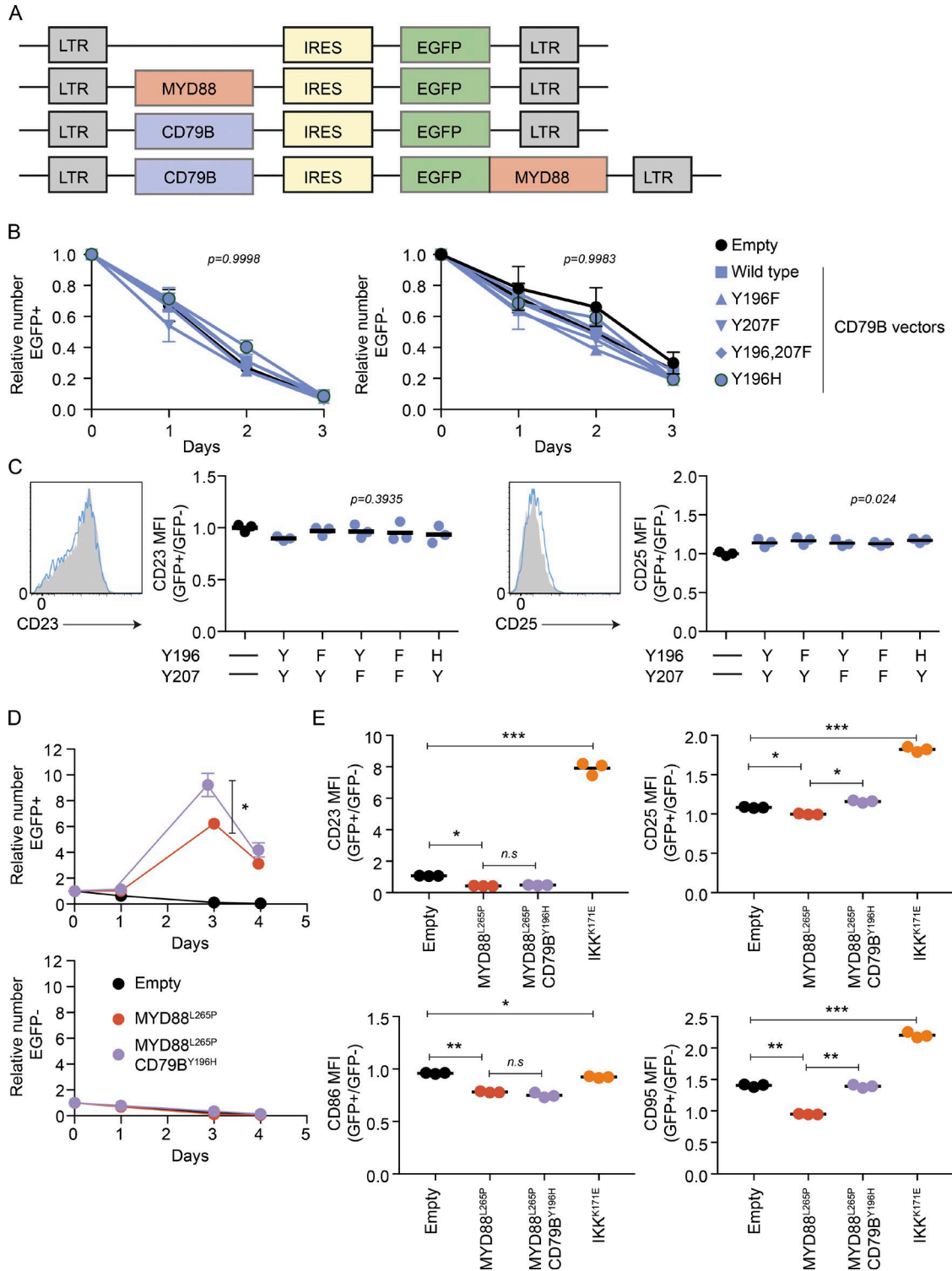


Figure 1. **CD79B ITAM mutations do not drive B cell proliferation or NF- κ B activation.** (A) Retroviral vector design for introducing wild-type/mutant mouse *Myd88* and/or *Cd79b* into activated B cells. (B) MD4 spleen B cells were activated in vivo by a single HEL injection 6 h before isolating spleen cells and washing and culturing them with anti-CD40 antibody but no BCR ligand for a total of 60 h, with retroviral spinoculation after the first 24 h. After activation and retroviral transduction, the cells were washed free of residual anti-CD40 and cultured in medium alone for the indicated times before flow cytometric analysis. The mean and standard deviation number of EGFP⁺ cells expressing empty vector, wild-type CD79B, or the indicated mutant CD79B are expressed relative to the number on day 0 of the culture. (C) Representative histograms (empty vector in gray, wild-type CD79B in blue) and mean fluorescence intensity (MFI) of cell surface CD23 or CD25 on EGFP⁺ cells on day 1 of culture without anti-CD40, relative to the MFI of nontransduced

for surface IgM display: *Ighm* encoding IgM μ -heavy chains, *Igk* encoding κ -light chains, *Cd79a*, and *Cd79b*. These were analyzed in microarray datasets of whole transcriptomes from EGFP⁺ B cells sorted from two independent cultures expressing empty vector, MYD88^{L265P}, CARD11^{L232LI}, or IKK^{K171E} as previously described (Wang et al., 2014). As validation of the microarray data, *Myd88* mRNA was increased 800% in samples of MYD88^{L265P} transduced cells relative to all the other samples (Fig. 3 A). Consistent with the flow cytometric data in Fig. 1 E, the NF- κ B target gene *Fcer2a* encoding CD23 was decreased in MYD88^{L265P}-transduced cells relative to empty vector but increased in IKK^{K171E}-transduced cells. In contrast, MYD88^{L265P} did not decrease *Ighm* or *Igk* mRNA levels and only marginally decreased *Cd79a* and *Cd79b* (Fig. 3 A). To verify this result, EGFP⁺ cells expressing empty vector or MYD88^{L265P} were sorted from three independently transduced cultures of each, and cDNA was analyzed by quantitative PCR. This revealed increased *Myd88* mRNA in MYD88^{L265P}-transduced cells but no significant difference in *Ighm*, *Cd79a*, or *Cd79b* mRNA (Fig. 3 B).

Because the decreased surface IgM could not be explained by changes at the mRNA level, we used Western blotting of sorted EGFP⁺ cell lysates to measure the relative amounts of CD79B and IgM proteins in the pre-Golgi or post-Golgi compartments. N-linked glycans on newly synthesized (immature) CD79B and IgM μ -chains constitute high-mannose chains that can be cleaved by endoglycosidase H (Endo H), resulting in a shift to a lower molecular weight in SDS-PAGE. The N-linked carbohydrates are modified and become resistant to Endo H once the mature IgM-CD79A/B complex is assembled and transported through the trans-Golgi (Bell and Goodnow, 1994). Protein extracts from transduced and sorted EGFP⁺ B cells were treated with Endo H for 1 h at 37°C or mock-treated, followed by separation on SDS-PAGE and Western blotting with antibodies against CD79B, μ -chain, and tubulin. In B cells expressing empty vector, most of the CD79B and IgM μ -chain was in the mature, slowly migrating, Endo H-resistant form (Fig. 3 C). In contrast, in B cells expressing MYD88^{L265P} alone, IgM μ -chains were mostly immature and Endo H-sensitive, and these accumulated markedly (Fig. 3, C and D). In the same lysates, there was little change in the pool of immature CD79B, but there was a decrease in mature Endo H-resistant CD79B (Fig. 3, C and D). The pool of immature CD79B protein was increased in cells transduced with the *CD79B* vector, and coexpression of *CD79B*^{WT} with MYD88^{L265P} resulted in a higher proportion of μ -chains in the mature form and a decrease in the immature

μ -chain pool (Fig. 3, C and D). Collectively, the mRNA and Western blotting analysis indicates that MYD88^{L265P} triggers a post-translational block in IgM receptor trafficking to the trans-Golgi, resembling the trafficking block that explains low surface IgM in anergic self-reactive B cells (Bell and Goodnow, 1994). This IgM trafficking “checkpoint” could be relieved by increasing the pool of nascent CD79B protein, although future studies will need to determine how the increase in CD79B reverses the effects of MYD88^{L265P}.

Effect of MYD88^{L265P} on B cell transcriptome

The wider transcriptional effects of MYD88^{L265P} were explored by analyzing the microarray datasets described above using the limma package (Ritchie et al., 2015), focusing on well-annotated genes with Entrez IDs. Using CAMERA, a competitive test of enrichment suitable for small sample sizes and resistant to intergene correlation (Wu and Smyth, 2012), we first queried for enrichment of differentially expressed genes against predefined sets of hallmark, curated, and immunological signature gene sets defined in MSigDB (Table S1; Subramanian et al., 2005). We focused on evidence for differential expression between MYD88^{L265P}- and CARD11^{L232LI}-transduced B cells because both cell populations were actively proliferating at the time of RNA isolation, unlike empty vector-transduced cells, and because *CD79B* mutations appear to be coselected with MYD88^{L265P} in human lymphomas but not obviously with *CARD11* mutations.

Hallmark gene set M5890, comprising 207 genes regulated by NF- κ B in response to TNF, was one of three hallmark gene sets most significantly enriched for differentially expressed genes between MYD88^{L265P}- and CARD11^{L232LI}-expressing B cells (false discovery rate [FDR] = 7.78×10^{-6} ; Table S2). The majority of NF- κ B-induced mRNAs in this set were decreased in MYD88^{L265P}-expressing B cells (Fig. 4 A), consistent with our previous evidence that MYD88^{L265P} in transduced B cells induces negative feedback inhibition of NF- κ B through TNFAIP3 (Wang et al., 2014).

Gene set M1487, comprising 55 genes that are up-regulated in plasma cells relative to other B cell developmental stages (Mori et al., 2008), was one of two curated gene sets most significantly enriched for differentially expressed genes between MYD88^{L265P}- and CARD11^{L232LI}-expressing B cells (FDR = 1.68×10^{-12} ; Table S3). The majority of the plasma cell up-regulated gene set was increased in MYD88^{L265P}-expressing cells (Fig. 4 B). This set was one of the four most significantly enriched gene sets of all queried sets in MSigDB (Table S1). The three other gene sets with

EGFP⁻ control cells in the same culture, measured in independent triplicate cultures. Cells were transduced with vectors encoding no CD79B (-) or CD79B with the indicated substitutions at Tyr 196 or Tyr207. Statistical analysis by ANOVA. (D) Mean and SD number of EGFP⁻ or EGFP⁺ cells transduced with the indicated vectors and cultured without anti-CD40 relative to the number on day 0 of the same culture. (E) CD23, CD25, CD86, and CD95 MFI on EGFP⁺ cells expressing the indicated vectors in independent triplicate cohorts of cells relative to MFI of nontransduced EGFP⁻ cells after 1 d of culture without anti-CD40. Statistical analysis by ANOVA with Tukey's positive test comparing the indicated groups: *, P < 0.05; **, P < 0.01; ***, P < 0.001. Data are representative of at least three independent experiments.

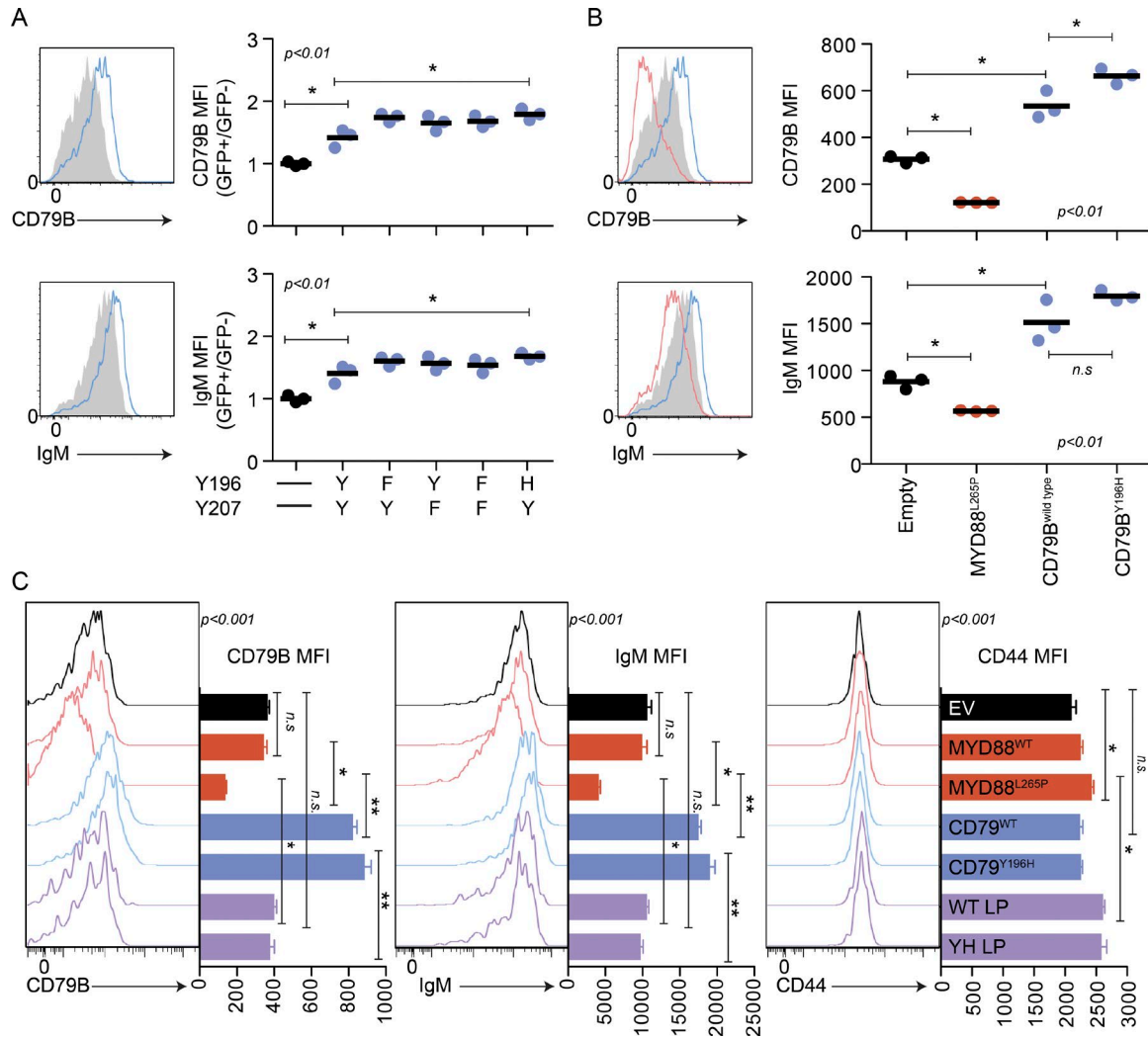


Figure 2. CD79B and MYD88 mutations have opposing effects on surface BCR expression. Spleen cells from C57BL/6 mice were cultured for 24 h with anti-IgM and anti-CD40 to activate B cells. Activated B cells were then washed, spinoculated with retroviral supernatants, and cultured for a further 36 h with anti-IgM and anti-CD40. The transduced cells were then washed free of residual anti-IgM and anti-CD40 and placed into fresh triplicate cultures without any mitogen for 24 h before staining with antibodies to cell surface CD79B and IgM and flow cytometry. (A) Representative histograms and graphs displaying mean fluorescence intensity (MFI) of surface CD79B or IgM on EGFP⁺ cells in independent cultures of cells transduced with EGFP only empty vector (gray) or vectors encoding wild-type or indicated mutant CD79B (blue). In the graphs, the MFI for each cohort of EGFP⁺ cells is expressed relative to the MFI of nontransduced EGFP⁻ control cells in the same culture. (B and C) Representative histograms (red, MYD88; blue, CD79B; purple, dual CD79B and MYD88) and MFI of EGFP⁺ B cells transduced with the indicated vectors and staining for cell surface CD44 as a control protein not part of the BCR complex. EV, empty vector. Graphs in C show means and SDs of EGFP⁺ cells in independent triplicate cultures. Data are representative of two independent experiments. Statistical analysis by ANOVA with Tukey's positive test comparing the indicated groups: *, P < 0.05; **, P < 0.01.

comparably small FDR values all constitute genes increased in myeloid cell differentiation, which were decreased in MYD88^{L265P}-expressing cells.

When the transcriptome of MYD88^{L265P}-expressing B cells was compared with empty vector-expressing B cells using limma, 111 genes had strong evidence for differential expression with 88 increased in MYD88^{L265P} cells (Fig. 4 C and Table S4). Compared with CARD11^{L232L1}-expressing B cells, 84 genes had strong evidence for differential expression in MYD88^{L265P} B cells, with 30 increased, including the plasma

cell-induced genes *Prdm1* and *Igj* (J-chain; Fig. 4 D). Comparing MYD88^{L265P} B cells with all the other groups yielded 22 probe sets with strong evidence of differential expression in MYD88^{L265P}-transduced cells relative to all the other cell types examined, and all were increased in MYD88^{L265P} cells. Ranked by fold change relative to CARD11^{L232L1}-expressing cells, they were *Hnflb*, *Tmed6*, *Myd88*, *Mybl1*, *Pcbd1*, *Map2*, *Nqo1*, *Gm10558*, *Prdm1*, *Chac2*, *Rnd3*, *Ccl3*, *Tnip3*, *Fam46c*, *Ccr9*, *Ehf*, *Cdc14b*, *Slco4c1*, *Depdc7*, *Sfnbt2*, *Fam81a*, and *Fam135a*. *Myd88* was expected on the basis of the analysis

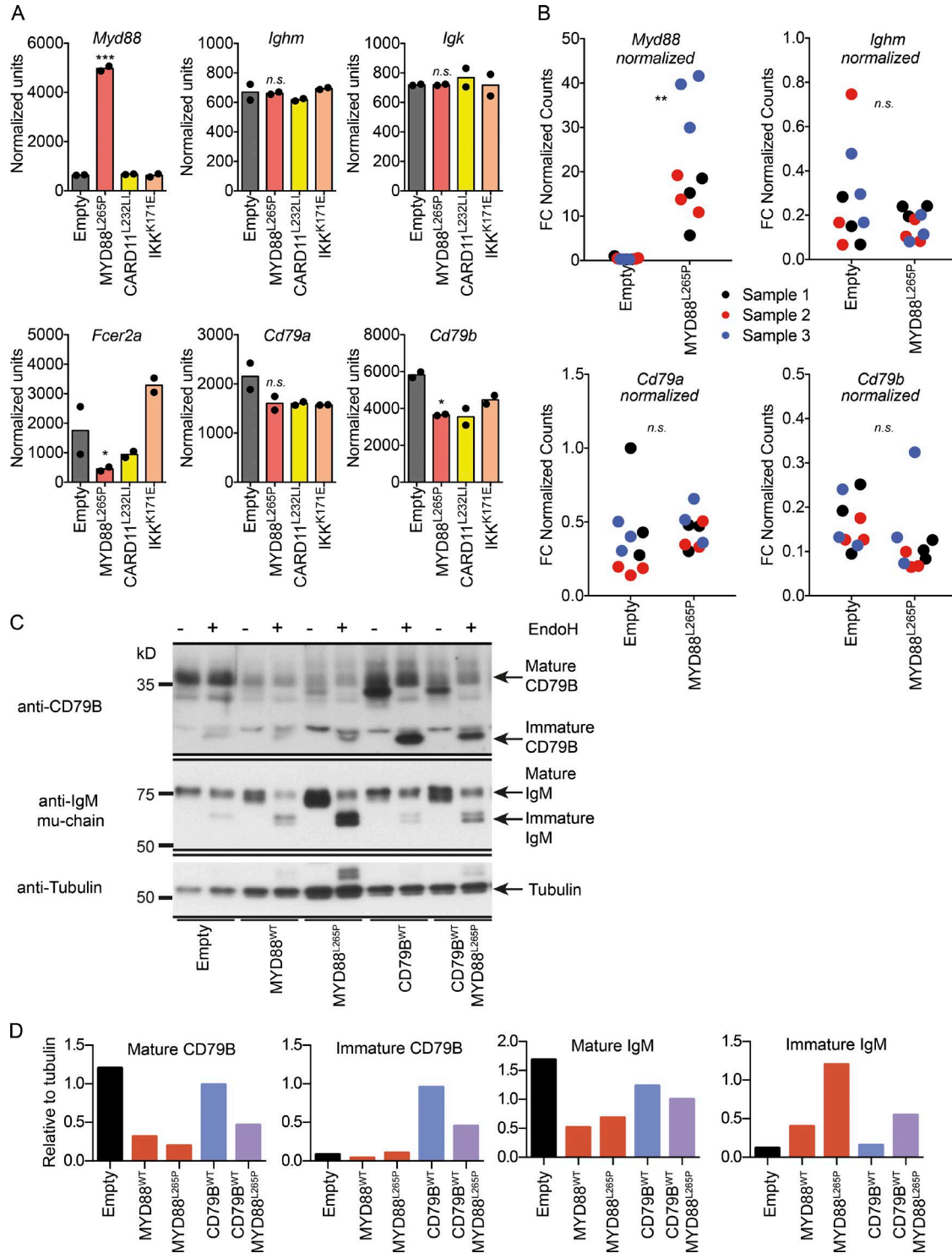


Figure 3. ***MYD88*^{L265P} mutation down-regulates surface IgM by inhibiting intracellular BCR maturation.** (A) After activation, transduction, washing free of anti-CD40, and 24-h culture without mitogen, EGFP⁺ B cells expressing empty vector (EV), MYD88^{L265P}, CARD11^{L232LL}, or IKK^{K171E} were sorted from $n = 2$ independent cultures for B cells expressing each vector type. RNA was isolated and analyzed on Affymetrix microarrays. Shown is normalized signal in arbitrary units for *Myd88*, *Ighm*, *Igk*, *Fcer2a* (CD23), *Cd79a*, and *Cd79b*. Statistical analysis by one-way ANOVA with Tukey's positive test comparing the indicated groups with EV cells: *, $P < 0.05$; ***, $P < 0.001$. (B) Quantitative PCR quantitation of *Myd88*, *Ighm*, *Cd79a*, and *Cd79b* mRNA in EGFP⁺ cells expressing EV or MYD88^{L265P} sorted from an independent set of triplicate cultures (denoted by different colors) and measured in triplicate. Statistical analysis by Student's t test: **, $P < 0.01$. (C) EGFP⁺ B cells expressing the indicated vectors were sorted after 1-d culture without anti-CD40 (2.5 d since last exposure to

above (Fig. 3), validating the limma analysis. *Tnip3* encodes a negative regulator of NF- κ B that interacts with TNFAIP3 (Verstrepen et al., 2014). *Fam46c* is a member of the curated plasma cell up-regulated gene set M1487 (Mori et al., 2008) and is frequently deleted or mutated in human multiple myeloma (Lohr et al., 2014).

MYD88^{L265P} and CD79B mutations cooperatively drive plasmablast differentiation

Because B cell receptor signaling is critical for B cell survival and differentiation in vivo, we next asked if the *CD79B*^{Y196H} mutations would allow differentiation of *MYD88*^{L265P}-expressing B cells into plasmablasts when transplanted into *Rag1*-deficient mice, as observed for cells expressing single gain-of-function *CARD11* mutations (Jeelall et al., 2012). Plasmablast differentiation from polyclonal C57BL/6 B cells could theoretically have been driven by BCRs that bound to self- or microbe antigens; therefore for these experiments we used HEL-specific B cells from MD4 transgenic mice that received no BCR stimulation after retroviral transduction and transplantation in vivo. HEL and anti-CD40 activated B cells were transduced with *CD79B* and/or *MYD88* vectors, washed, and transplanted into *Rag1*^{-/-} recipient mice and analyzed in the spleen after 11 d.

Gating on the EGFP⁺ subset of transferred B cells revealed that those expressing *CD79B*^{WT} *MYD88*^{L265P} or *CD79B*^{Y196H} *MYD88*^{L265P} vectors accumulated in greater numbers and had lower CD19 and B220 expression compared with B cells expressing *MYD88*^{L265P} alone (Fig. 5, B–E). CD19 and B220 are two B cell lineage markers that are repressed upon differentiation into plasma cells (Nutt et al., 1998). CD19 and B220 down-regulation on *CD79B*^{Y196H} *MYD88*^{L265P} B cells paralleled the phenotype of *Thr9*^{-/-} *MYD88*^{L265P} B cells that undergo plasmablast differentiation after transplantation to *Rag1*^{-/-} recipients (Wang et al., 2016) and B cells transduced with gain-of-function *CARD11* mutation (Jeelall et al., 2012). After correcting for the number of EGFP⁺ cells transplanted on day 0 (Fig. 5 A), *MYD88*^{L265P} B cells were present in 5-fold higher number than empty vector B cells on day 11, and *CD79B*^{WT} *MYD88*^{L265P} or *CD79B*^{Y196H} *MYD88*^{L265P} B cells accumulated to 8- and 15-fold higher numbers, respectively (Fig. 5 C).

Plasma cell differentiation was further analyzed by transducing polyclonal C57BL/6 B cells, transplanting them into *Rag1*^{-/-} recipients, and analyzing the recipients 11 d later (Fig. 5, F–I). CD19 was significantly decreased on IgM⁺ EGFP⁺ cells coexpressing *MYD88*^{L265P} with *CD79B* or *CD79B*^{Y196H}

compared with control cells expressing only one or other protein (Fig. 5 F). In contrast, surface IgM was increased on the cells coexpressing *MYD88*^{L265P} with *CD79B* or *CD79B*^{Y196H} compared with cells expressing *MYD88*^{L265P} alone, the latter having lower surface IgM than empty vector-expressing B cells (Fig. 5 G). Down-regulation of CD19 was accompanied by induction of CD138 and by secretion of large amounts of serum IgM in recipients of cells coexpressing *MYD88*^{L265P} with *CD79B* or *CD79B*^{Y196H} (Fig. 5, H and I; and Fig. S2). Interestingly, there was no detectable secretion of IgG, indicating that the cooperation between *MYD88*^{L265P} and *CD79B* drives plasma cell differentiation but not isotype switching to IgG. These results are similar to the down-regulation of CD19 and B220, induction of CD138, and secretion of IgM but not IgG by C57BL/6 B cells expressing *MYD88*^{L265P} combined with TLR9-deficiency (Wang et al., 2016).

Abnormal CD79B and MYD88^{L265P} cooperatively break tolerance checkpoints

Gain-of-function *CARD11* mutations derived from human lymphomas disrupt several B cell tolerance checkpoints when introduced into activated mouse B cells, switching the effect of self-antigen from inducing apoptosis into induction of proliferation and plasmablast differentiation and autoantibody secretion (Jeelall et al., 2012). Using the same experimental system, *MYD88*^{L265P} did not protect B cells from self-antigen-induced deletion unless combined with enforced BCL2 expression, and the *MYD88*^{L265P} *BCL2* combination remained insufficient to break tolerance checkpoints that oppose plasmablast differentiation and autoantibody secretion (Wang et al., 2014). Hence we used the identical experimental model to test if cooperation between *CD79B* and *MYD88* mutations would override peripheral tolerance checkpoints in self-antigen-binding B cells transferred to antigen-expressing recipient mice. Mature MD4 Ig^{HEL}-transgenic B cells bearing HEL-specific BCRs were activated, transduced with the *CD79B* and *MYD88* single or combined retroviral vectors, and transplanted into ML5-transgenic *Rag1*^{-/-} recipient mice that expressed HEL protein in their circulation as self-antigen (Goodnow et al., 1988).

The number of surface HEL-binding IgM⁺EGFP⁺ B cells was measured at the time of transplantation (input) and in the spleen of the recipients 11 d after transplantation (Fig. 6, A and C). Retrovirally transduced EGFP⁺ B cells expressing no additional protein or only *MYD88*^{L265P} were eliminated by self-tolerance, as were EGFP⁺ B cells expressing only *CD79B*^{WT} or *CD79B*^{Y196H} (Fig. 6, B and

anti-CD40 or anti-IgM). Cell lysates were treated with Endo H or buffer only before SDS-PAGE and Western blotting with antibodies against mouse CD79B, IgM μ -chain, and tubulin as a loading control. Arrows indicate position of immature CD79B or μ -chain after Endo H cleavage of high-mannose N-glycans and slower migrating mature proteins with complex N-glycans resistant to Endo H. (D) Densitometry analysis of the Western blot in C, showing the relative abundance of mature Endo H-resistant and immature Endo H-sensitive CD79B and μ -chains compared with tubulin loading control in each sample. Data are representative of three independent experiments.

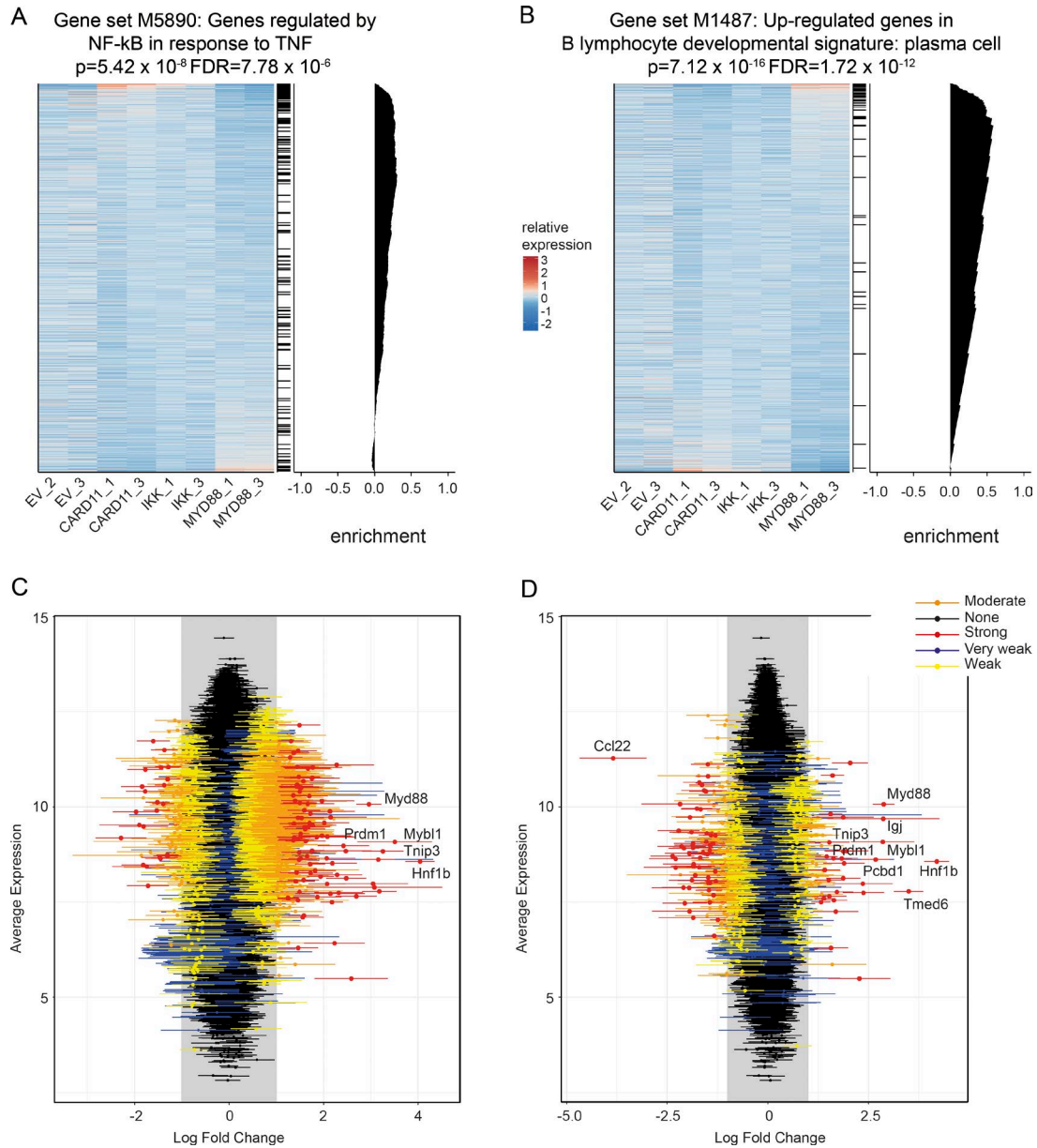


Figure 4. **Effect of MYD88^{L265P} on global RNA expression in B cells.** Global analysis using limma of the RNA Affymetrix microarray dataset in Fig. 3 A, from two independent cultures of EGFP⁺ cells expressing empty vector, MYD88^{L265P}, CARD11^{L232LI}, or IKK^{K171E}. (A and B) CAMERA, a competitive test of enrichment suitable for small sample sizes and resistant to intergene correlation, was implemented in the limma package to test the entire dataset for enrichment of hallmark, curated, and immunological signatures gene set defined in MSigDB. Shown are (A) the third most significantly enriched hallmark gene set and (B) the second most significantly enriched curated gene set. A complete list of enriched gene sets is provided in Table S1. (C and D) The limma package was used to compare normalized RNA signals in MYD88^{L265P}-expressing cells with (C) empty vector-expressing cells or (D) CARD11^{L232LI}-expressing cells. The y-axis shows the mean expression signature for each probe set across all eight samples; the x-axis shows the mean and 95% confidence interval for the fold change in expression of each probe set in MYD88^{L265P} cells compared with (C) empty vector cells and (D) CARD11^{L232LI} cells. Probe sets are color-coded by strength of evidence for differential expression, and those with highest fold change are marked with corresponding gene symbol.

C), indicating that the CD79B ITAM mutation on its own did not disrupt this tolerance checkpoint. In contrast, B cells coexpressing CD79B^{WT} or CD79B^{Y196H} with MYD88^{L265P} were protected from self-antigen-induced deletion (Fig. 6, B and C). On average, 10 to 30 times more EGFP⁺ cells

accumulated when the transplanted B cells were CD79B^{WT} MYD88^{L265P} or CD79B^{Y196H} MYD88^{L265P}, respectively, compared with recipient mice that received B cells expressing only one or other mutant protein (Fig. 6 C). Inhibiting the peripheral deletion checkpoint therefore required co-

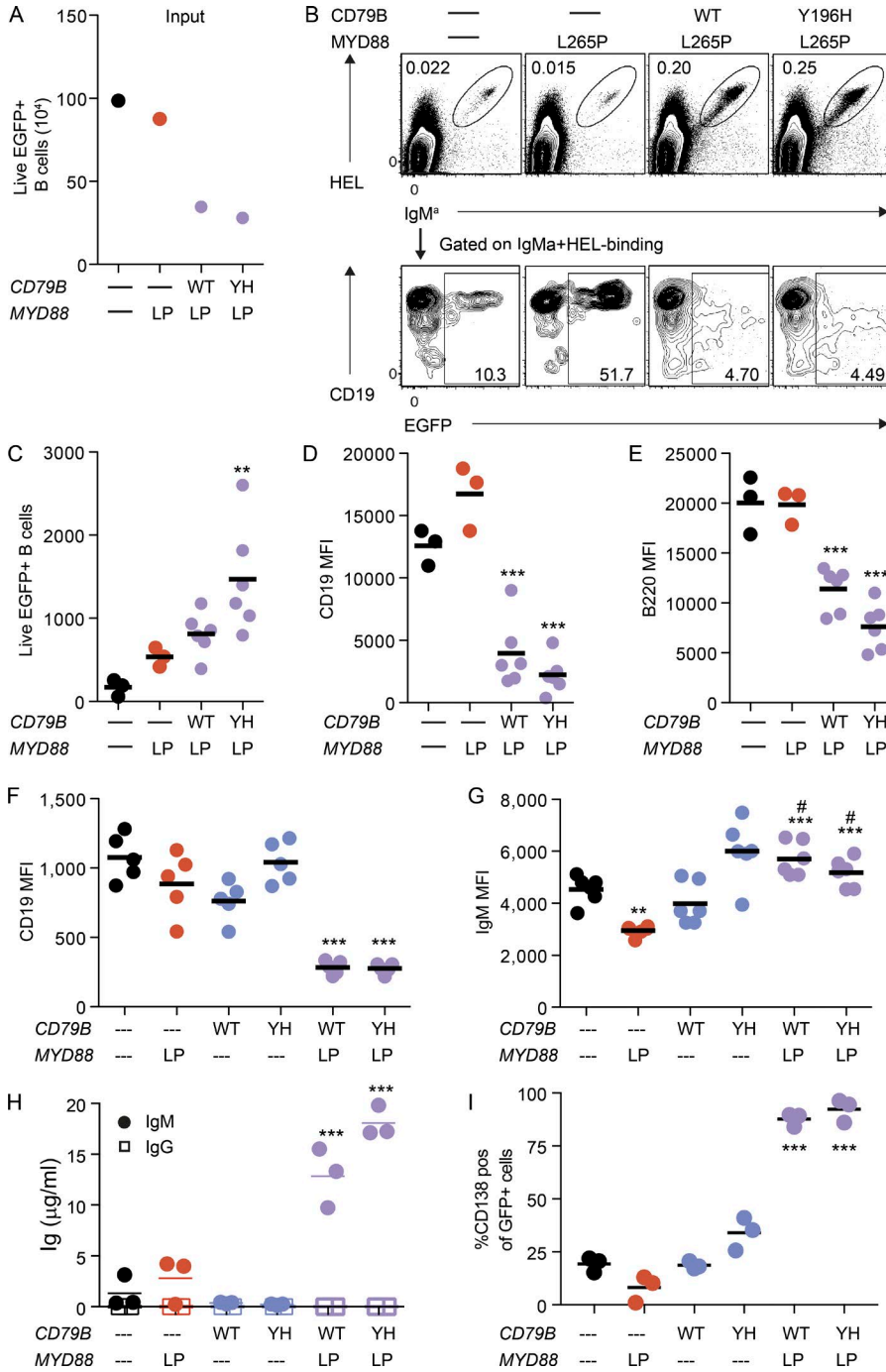


Figure 5. *MYD88*^{L265P} and *CD79B* mutations cooperate to promote plasmablast differentiation. (A–E) MD4 transgenic B cells were transduced with empty vector or vectors expressing *MYD88*^{L265P} alone (LP) or combined with wild-type *CD79B* (WT) or *CD79B*^{Y196H} (YH). (A) Number of live EGFP⁺ B cells, each cell likely to represent an independent transduction event, transplanted into each *Rag1*^{-/-} recipient mouse. (B) Flow cytometric analysis of the spleen of recipient mice 11 d after transplantation, showing concatenated data from three to five recipients per treatment. Top row: mean percentage of IgM⁺ HEL-binding donor-derived B cells among live leukocytes; bottom row: mean percentage of EGFP⁺ cells among IgM⁺ HEL-binding cells and CD19 expression on these cells. (C) Number of live EGFP⁺ B cells in the spleen of individual recipients 11 d after transplantation. Bars denote arithmetic means. (D and E) Mean fluorescence intensity (MFI) of CD19 and B220 measured on IgM⁺ HEL-binding EGFP⁺ B cells. Data are representative of three independent experiments. (F–I) C57BL/6 B cells were transduced with the indicated vectors and transplanted into *Rag1*^{-/-} mice. Eleven days later, IgM⁺ EGFP⁺ cells were analyzed in the spleen, measuring MFI of (F) CD19 and (G) MFI of cell surface IgM in individual recipients. Data are representative of two independent experiments. (H) At the same time, serum IgM (circle) and IgG (square) were measured in individual recipients. (I) The percentage of IgM⁺ EGFP⁺ cells expressing CD138 was measured in a separate experiment (Fig. S2). Statistical analysis by ANOVA with Tukey's positive test comparing the indicated groups with empty vector and *MYD88*^{L265P} cells (**, *P* < 0.01; ***, *P* < 0.001) or comparing with EV only, #, not statistically significant.

operation between dysregulated *CD79B* and *MYD88*^{L265P}. Moreover, self-reactive B cells coexpressing *CD79B*^{WT} *MYD88*^{L265P} or *CD79B*^{Y196H} *MYD88*^{L265P} differentiated into CD19^{low} plasmablasts (Fig. 6 B). Analysis of the serum from the recipients by ELISA showed secreted anti-HEL autoantibodies only in recipients of B cells with dysregulated *CD79B* and mutant *MYD88* (Fig. 6 D), indicating that cooperation between the mutations caused a potent disruption to B cell tolerance checkpoints.

Break of B cell tolerance by combining *CD79B* and *MYD88* mutations correlates with surface BCR levels

Transcription of *CD79B*^{WT} from the retroviral promoter increased CD79B and IgM on the surface of transduced B cells to a similar amount compared with the *CD79B* ITAM mutation (Fig. 2, A and B) and increased the pool of pre-Golgi Endo H-sensitive CD79B (Fig. 3 C). We therefore sought to diminish translation of the retroviral *CD79B* transcript with the aim of distinguishing the effect of

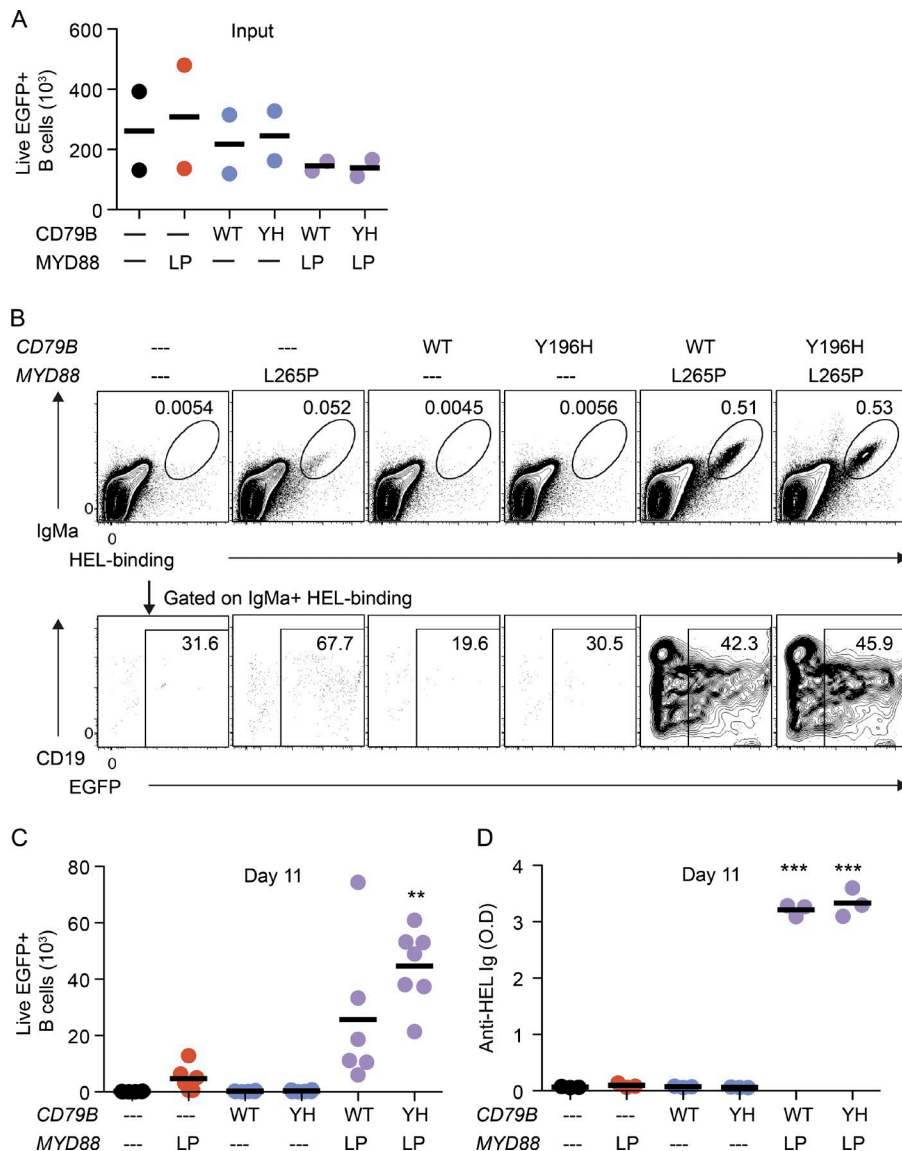


Figure 6. Combined *MYD88*^{L265P} and *CD79B* mutations break B cell tolerance to self-antigen in vivo. (A) Number of live EGFP⁺ MD4 Ig^{HEL}-transgenic B cells transduced with EGFP vectors encoding the indicated additional proteins (-, no *CD79B* or *MYD88* protein; WT, wild-type protein; LP, L265P; YH, Y196H) transplanted into each ML5 HEL-transgenic *Rag1*^{-/-} recipient mouse in two independent experiments. (B) Flow cytometric analysis of the spleen of recipient mice 11 d after transplantation, showing concatenated data from three recipients per treatment. Top: percentage of IgM⁺ HEL-binding donor-derived B cells among live splenic leukocytes; bottom: mean percentage EGFP⁺ cells among IgM⁺ HEL-binding donor B cells and CD19 expression on these cells. (C) Number of live EGFP⁺ IgM⁺ HEL-binding B cells in the spleen of each recipient mouse. Data are pooled from two independent experiments, each with *n* = 3 or 4 per group. Bar denotes arithmetic mean. (D) HEL-binding IgM antibody in serum of individual recipients, measured by ELISA. O.D., optical density. Statistical analysis by ANOVA with Tukey's positive test comparing the indicated groups with empty vector (EV) and *MYD88*^{L265P} cells: **, *P* < 0.01; ***, *P* < 0.001.

CD79B^{Y196H} from that of *CD79B*^{WT}. *CD79B* translation was diminished by introducing one of six different upstream open reading frames into the 5' untranslated region (5' UTR) of the *CD79B* coding sequence (Fig. S1; Calvo et al., 2009). When cell surface *CD79B* was measured on the transduced B cells with the same level of EGFP expression, the 5' UTR variants decreased the *CD79B* mean fluorescence intensity compared with B cells expressing the *CD79B*^{WT} with the typical Kozak sequence (Fig. 7 A). Two 5' UTR sequences were also tested for their effects on surface IgM expression. Whereas surface IgM and *CD79B* were twice as high on EGFP⁺ cells expressing *CD79B*^{WT} cDNA compared with cells expressing the control EGFP vector alone, both were decreased to levels comparable with the control cells when the *CD79B*^{WT} cDNA carried the *UTR4* insertion and were increased by only 35% when the *UTR6* insertion was present (Fig. 7 B).

To test the effects of these translationally dampened *CD79B* vectors on peripheral B cell tolerance checkpoints, we transduced HEL-specific B cells with the *CD79B*^{WT} *MYD88*^{L265P} or *CD79B*^{Y196H} *MYD88*^{L265P} vectors preceded by *UTR4* or *UTR6* and transplanted the B cells into HEL-transgenic mice as before (Fig. 7 C). After 5 d, HEL-specific EGFP⁺ B cells expressing empty vector, *MYD88*^{L265P} alone, *CD79B*^{WT} alone, or *CD79B*^{Y196H} alone did not persist in the recipient mice expressing HEL antigen, but B cells expressing the *CD79B*^{WT} *MYD88*^{L265P} or *CD79B*^{Y196H} *MYD88*^{L265P} vectors resisted deletion to varying extents (Fig. 7 D). On average, twice the number of EGFP⁺ B cells persisted when they expressed the higher expression *UTR6* vector compared with the *UTR4* vector (Fig. 7 D). Furthermore, B cells expressing the *UTR6* *CD79B*^{Y196H} *MYD88*^{L265P} vector preferentially accumulated on average to twice the number of B cells expressing *UTR6* *CD79B*^{WT}

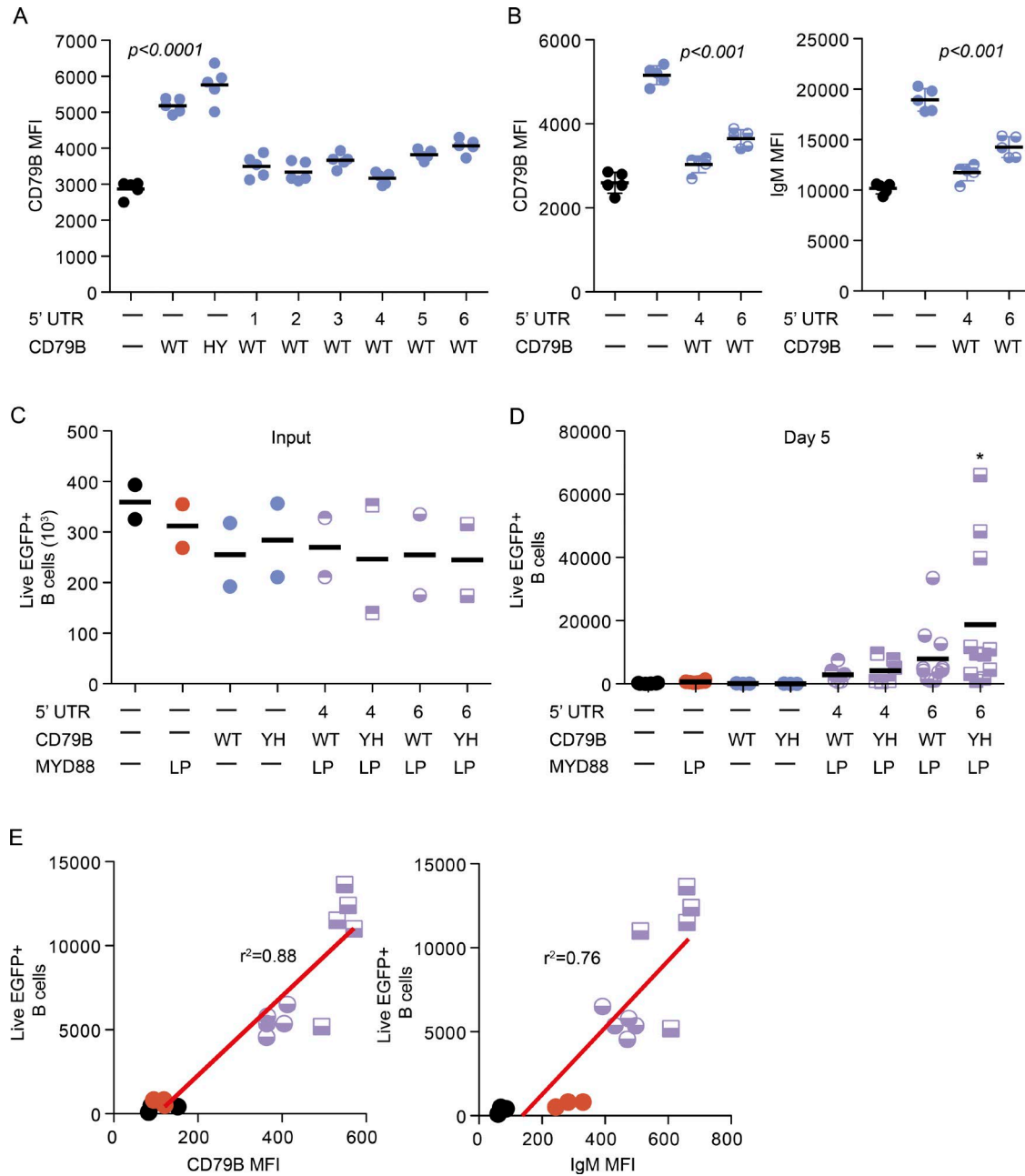


Figure 7. Checkpoint inhibition by *CD79B* and *MYD88* mutations correlates with amount of surface BCR expressed. (A) MD4 HEL-specific B cells were activated and transduced with bicistronic EGFP retroviral vectors encoding no additional protein (-), *Cd79b*^{WT} with normal 5' UTR, *Cd79b*^{Y196H} (YH), or *Cd79b*^{WT} with one of six different open reading frame insertions in the *Cd79b* 5' UTR (5' UTR1-6; Fig. S1). After washing, *n* = 5 independent cultures of cells transduced with each vector were established without antigen or CD40 stimulation and analyzed 24 h later by flow cytometry for cell surface CD79B mean fluorescence intensity (MFI) gated on cells expressing equivalent level of EGFP. Bars denote arithmetic means. Statistical analysis by one-way ANOVA with Tukey's positive test comparing the indicated groups. (B) Independent experiment as in (A), analyzed for cell surface CD79B and IgM. (C-E) HEL-specific B cells were transduced with vectors encoding *Myd88*^{L265P}, *Cd79b*^{WT}, *Cd79b*^{Y196H}, without or with the 5' UTR 4 or 6 insertions. The cells were transplanted to HEL-transgenic *Rag1*^{-/-} recipients. (C) Number of EGFP⁺ B cells transplanted into each recipient mouse; *n* = 2 independent experiments. (D) Number of EGFP⁺ B cells in the spleen of each recipient 5 d after transplantation. Data are pooled from two independent experiments, each with *n* = 3-5 recipients per group. Bars are arithmetic means. Statistical analysis by ANOVA with Tukey's positive test comparing the indicated groups with empty vector and *MYD88*^{L265P} cells; *, *P* < 0.05. (E) Number of EGFP⁺ B cells in each recipient plotted against the mean fluorescence intensity of CD79B and IgM on the EGFP⁺ cells in the same mouse at the time of enumeration. Symbols as in D. Statistical analysis by linear regression. Data are representative of two independent experiments.

MYD88^{L265P} (Fig. 7 D). Although the number of self-reactive EGFP⁺ B cells resisting deletion was variable, it was strongly correlated with their surface CD79B and IgM expression in the recipient mice (Fig. 7 E), indicating that escape from self-tolerance by *MYD88^{L265P}* B cells required increased BCR expression through cooperation with alterations in CD79B.

DISCUSSION

CD79B and *MYD88* mutations frequently occur together in mature B cell malignancies. Here we reveal that they cooperate synergistically to induce B cell differentiation into plasmablasts and break self-tolerance checkpoints in B cells within peripheral lymphoid tissue. What might be the basis for the striking cooperation between *CD79B* and *MYD88* mutations in our experiments?

Several lines of evidence here support a conclusion that surface BCR density is governed by CD79B and represents a critical, rate-limiting factor for B cells expressing *MYD88^{L265P}*. First, CD79B appears to be the rate-limiting component for surface BCR expression in normal B cells, because retrovirally increasing the expression of *CD79B* increased the mean surface IgM to 150% of controls, and this could be further increased if the retrovirally expressed *CD79B* carried tyrosine substitutions in the membrane proximal ITAM found recurrently in human lymphomas (Davis et al., 2010). Second, B cells expressing *MYD88^{L265P}* down-regulate their surface CD79B and IgM despite having no decrease in mRNA for all four essential components of surface IgM BCRs. Low surface IgM expression in *MYD88^{L265P}* B cells is instead explained by accumulation of immature, pre-Golgi, Endo H-sensitive IgM, representing a “checkpoint” remarkably similar to the posttranslational block to surface IgM expression induced by chronic binding to self-HEL antigen (Bell and Goodnow, 1994). Hence it is conceivable that the expression of *MYD88^{L265P}* and chronic exposure to self-antigen act additively or cooperatively to block surface BCR trafficking and accumulation on the cell surface, which may deprive the cells of tonic BCR survival signals to counter B cell apoptosis *in vivo*. The third line of evidence that CD79B represents a critical limiting factor in B cells expressing *MYD88^{L265P}* comes from the experiment introducing 5' UTR open reading frames that compete with the normal translation initiation of retrovirally encoded CD79B protein. The decrease in CD79B and IgM surface display was correlated with a decrease in the capacity of CD79B to block deletion of HEL-specific B cells when combined with *MYD88^{L265P}*. In this case, the rescue of mature B cells from self-antigen induced deletion was enhanced by Y196H mutation and correlated with increased surface CD79B and IgM.

Previous studies have shown that the deletion of HEL-specific B cells in HEL-transgenic mice is preceded by down-regulation of surface IgM and is mediated by apoptosis that is inhibited by *Bcl2* overexpression (Cyster et al., 1994) and requires the BCL2 antagonist BIM (Enders et al., 2003). When the capacity to synthesize surface IgM is experimen-

tally ablated by conditional gene deletion, mature B cells undergo apoptosis in FOXO1-dependent and BIM-dependent manner that is also inhibited by enforced expression of BCL2 (Lam et al., 1997; Srinivasan et al., 2009). B cells that lose surface IgM have decreased phosphorylation of AKT, an intermediate in phosphoinositide 3-kinase (PI3K) inhibition of FOXO1, and can be protected against apoptosis by mutations that constitutively activate PI3K (Srinivasan et al., 2009). Conversely, exaggerated surface IgM accumulation and increased AKT activation occurs in B cells with substitutions in both ITAM tyrosines in CD79B (Gazumyan et al., 2006). These results are consistent with the view that surface IgM paired with CD79A and CD79B, in the absence of antigen, continuously signals through the ITAMs in CD79A to activate PI3K at a tonic level and thereby activate AKT, inhibit FOXO1 accumulation, and repress BIM formation in B cells to promote their survival. Thus, the BIM-dependent deletion of HEL-specific B cells that follows self-antigen-induced BCR down-regulation may therefore result, at least in part, from the loss of surface BCR CD79A tonic signaling to PI3K. Because *MYD88^{L265P}* decreases surface BCR even in the absence of self-antigen, any prosurvival signal induced by *MYD88^{L265P}*, for example through the activation of NF- κ B, may be overwhelmed by the loss of surface BCR and its PI3K survival signal. Our previous work showing the striking cooperation between *Bcl2* overexpression and *MYD88^{L265P}* for enhancing B cell survival both in the absence or presence of self-antigen supports the idea that the capacity of *MYD88^{L265P}* to promote B cell survival and proliferation is normally overwhelmed by BIM-mediated apoptosis (Wang et al., 2014).

Notably, overexpression of neither *CD79B^{WT}* nor *CD79B^{Y196H}* alone was sufficient to block self-antigen-induced deletion. One explanation is that preserving tonic BCR signaling to PI3K alone is insufficient to counter other inducers of apoptosis, including the elevation of BIM and Nur77 (Healy et al., 1997; Glynne et al., 2000; Zikherman et al., 2012). When *MYD88^{L265P}* is then coexpressed with *CD79B* vectors in self-reactive B cells, *MYD88^{L265P}*-IRAK signaling to activate NF- κ B may counter additional proapoptotic mediators by inducing prosurvival proteins such as BCL-XL and A1, which are not normally induced by self-antigen activation of the BCR (Glynne et al., 2000).

In addition to cooperating to block self-antigen-induced B cell deletion, the combination between *CD79B* and *MYD88* mutations also overrides the B cell tolerance checkpoint that normally inhibits TLR9- or TLR4-driven self-reactive B cell differentiation into CD19^{low} plasmablasts (Rui et al., 2003, 2006). This checkpoint is induced by chronic self-antigen engagement and BCR signaling to ERK (Rui et al., 2003, 2006). ERK phosphorylates and promotes the activity of an essential inhibitor of plasmablast differentiation, ETS1 (Bories et al., 1995; Hollenhorst et al., 2011). The promotion of plasmablast differentiation by CD79B was not simply a result of enhanced survival of self-reactive B cells, because overexpressing BCL2 enhances the accumulation of

MYD88^{L265P}-expressing B cells but not their differentiation into CD19^{low} plasmablasts (Wang et al., 2014).

The microarray data identified increased expression of plasma cell up-regulated genes in MYD88^{L265P}-expressing B cells compared with CARD11^{L232LI}-expressing B cells, raising the possibility that MYD88^{L265P} alone initiates an abortive plasma cell differentiation program that requires an additional signal from the BCR to be completed. Weaker gain-of-function alleles of CARD11 do not spontaneously drive B cell differentiation into plasmablasts unless the cells receive an additional BCR stimulus by binding self-antigen (Jeelall et al., 2012). Elevated surface BCR caused by CD79B mutations or overexpression could provide an additional signal through PI3K activation to drive plasmablast differentiation by down-regulating ETS1. Several independent observations support this hypothesis: (1) the activation of PI3K p100 delta subunit regulates autoantibody formation by marginal zone and B1 B cells (Durand et al., 2009), (2) constitutively active PI3K ensures mature B cell survival even in the absence of IgM (Srinivasan et al., 2009), and (3) PI3K activation is involved in reducing *Ets1* levels during plasma cell differentiation (Luo et al., 2014). Similar to enhanced BCR signaling by CD79B mutations, B cell differentiation into plasmablasts in mice is exaggerated by other mutations that dysregulate BCR signaling, including loss-of-function mutations in *Lyn*, *Ptpn6* (SHP1), and *Cd22*, resulting in lupus-like symptoms such as pathogenic autoantibody production (Chan et al., 1997; Gross et al., 2009; Luo et al., 2014). These observations are likely due to the loss of *Ets1* expression, because *Ets1* is controlled by BCR-mediated signals through PI3K, BTK, IKK, and JNK (Luo et al., 2014). Additionally, *Ets1* deficiency also leads to B cell hyper-responsiveness to TLR9 stimulation and TLR9-dependent autoimmunity in mice (Wang et al., 2005). Therefore, in future studies, it will be interesting to test if the observed phenotype in CD79B and MYD88 double-mutant B cells results from PI3K activation to down-regulate ETS1.

CD79B mutations are seen in only 30% of MYD88^{L265P} ABC-DLBCL and 15% of WM (Ngo et al., 2011; Poulain et al., 2013), suggesting that other mechanisms may exist to antagonize the MYD88^{L265P} effect on CD79B and IgM trafficking through the Golgi to the cell surface. Indeed, *Lyn* copy number loss is found in 60% of patients with WM (Hunter et al., 2014). Lymphoma B cells with the CD79B ITAM mutation show reduced *Lyn* activity, suggesting that the effect of CD79B ITAM mutation could also be achieved by *Lyn* deficiency (Davis et al., 2010). In mice, *Lyn* deficiency results in exaggerated B lymphoblast expansion, autoantibody production, and elevated sensitivity to BCR stimulation (Chan et al., 1997; Cornall et al., 1998). Additionally, *Lyn* deficiency in mice causes hypersensitivity to MYD88 signaling, and this MYD88-dependent signaling is crucial for autoimmunity (Lamagna et al., 2013, 2014). However, one might question why ABC-DLBCLs with CD79B and MYD88 mutations resist differentiation and cell cycle arrest. One clue comes from clinical observations that 23% of human DLBCL cases have

chromosome 11q24.3 gain to elevate *Ets1* and *Fli1* expression to antagonize B cell differentiation (Bonetti et al., 2013). Additional mechanisms of differentiation block in DLBCL come from the frequent inactivation of *PRDM1* in up to 24% of ABC-DLBCLs by chromosome 6q21–q22.1 deletion (Pasqualucci et al., 2006). Furthermore, 77% of these tumors lack the BLIMP1 protein despite the presence of *PRDM1* mRNA (Pasqualucci et al., 2006). Therefore, different disease outcomes could result from additional mutations among the average 20 or more protein-altering mutations B cells acquire, which includes CD79B and MYD88 mutations.

MATERIALS AND METHODS

Mice

Splenic B cells were collected from C57BL6 mice or MD4 mice bearing rearranged transgenic immunoglobulin gene encoding for HEL-specific antibodies (Ig^{HEL} transgenic; Goodnow et al., 1988). All mice were generated on a C57BL6 background or backcrossed to that background for greater than 10 generations and were housed in specific pathogen-free environment at the Australian Phenomics Facility, Australian National University. Donor mice were aged 8–16 wk at the time of the experiments. *Rag1*^{-/-} and *Rag1*^{-/-} ML5 transgenic mice that express soluble HEL (Goodnow et al., 1988) were used as recipients at ages 8–14 wk. All animals used in this study were cared for and used in accordance with protocols approved by the Australian National University Animal Experimentation Ethics Committee and the current guidelines from the Australian Code of Practice for the Care and Use of Animals for Scientific Purposes.

Retroviral vectors and packaging

Mouse *Cd79b* was amplified by Platinum Pfx DNA polymerase (Invitrogen) from mouse splenic cDNA and subcloned into pcDNA3.1(+) vector. PCR-based site-directed mutagenesis was used to introduce *Cd79b* mutations. Sequence-confirmed *Myd88* and *Cd79b* genes were then transferred into pMXs-IRES-GFP vectors (Kitamura et al., 2003) either individually or as dual-expression vectors (Fig. 1 A). To modulate protein translation, short open reading frames were inserted into the 5' UTRs of *Cd79b* coding sequence (Fig. S1). Retroviral vectors containing *Myd88* or *Cd79b* or dual *Myd88* and *Cd79b* were transfected into Phoenix ecotropic packaging cells (ATCC) using calcium phosphate precipitation (Swift et al., 2001). Supernatants containing retroviral particles were collected 48 and 72 h after transfection and frozen at -80°C until use.

Retroviral transduction of mature B cells

MD4 transgenic mice were given 5 mg HEL to provide a pulse of antigen to activate HEL-specific B cells 6 h before removing the spleen and preparing a single-cell suspension and washing twice with fresh complete RPMI by centrifugation at 300 g for 5 min at 8°C. Splenocytes were cultured at 4×10^6 cells/ml in complete RPMI containing 10

$\mu\text{g/ml}$ anti-CD40 antibody (FGK4.5; Bio X Cell) for 24 h. For splenocytes from nontransgenic C57BL/6 mice, 7 $\mu\text{g/ml}$ anti-IgM (Jackson ImmunoResearch Laboratories, Inc.) was also included during the initial 24-h activation culture. After 24 h, the cells were washed twice in RPMI and spin-infected in 6-well plates at 920 g for 90 min at room temperature with retrovirus supernatant containing 10 $\mu\text{l/ml}$ DOTAP (Roche). The cells were then placed back in fresh RPMI containing 10 $\mu\text{g/ml}$ anti-CD40 but no BCR ligands for HEL-specific B cells, or anti-CD40 plus 10 $\mu\text{g/ml}$ anti-IgM for nontransgenic B cells for 36 h. The transduced cells were then washed three times with fresh complete RPMI by centrifugation at 300 g for 5 min at 8°C, and any remaining media containing trace amount of anti-CD40 and/or anti-IgM antibodies was carefully removed. The number of live cells was determined by hemocytometer counting of Trypan blue–negative cells, and the percentage of EGFP⁺ 7AAD⁻ cells was determined by flow cytometry. Washed, transduced cells were then cultured in 24-well plates at 10⁶ cells/ml in fresh complete RPMI without anti-CD40 or BCR ligand, with the start of the mitogen-free cultures designated “day 0.”

Adoptive transfer and cell culture

Retrovirally transduced B cells were recovered 36 h after transduction and washed, and live cells were enumerated by Trypan blue exclusion. Live cells (2–10 $\times 10^6$), consisting of a mixture of transduced and nontransduced B cells, were transferred into each recipient mouse through lateral tail vein injection. Recipient mice were sacrificed after 5–11 d and their spleens analyzed for the amount of EGFP⁺ HEL-binding mature B cells. For cell culture experiments, cells were washed and cultured at 10⁶ cells/ml fresh RPMI media supplemented with 10% vol/vol FCS and 2% vol/vol penicillin, streptomycin, and glutamine without B cell mitogens in 24-well plates. The start of the cultures was designated “day 0.” The number of EGFP⁺ cells on the subsequent days in culture was then determined by hemocytometer counting of Trypan blue–negative cells and flow cytometric analysis of the percentage of EGFP⁺ 7AAD⁻ cells and expressed as relative amount compared with day 0.

Flow cytometric analysis

Single-cell suspensions were prepared and transferred to 96-well round-bottom plates. Cells were then incubated for 30 min at 4°C with antibody cocktails containing appropriate combination and dilution of antibodies in flow cytometry buffer (PBS with 2% vol/vol bovine serum and 0.1% wt/vol sodium azide). Cells were then washed twice and resuspended in flow cytometric buffer containing 7AAD for analysis on an LSR II or LSR Fortessa flow cytometer (BD). The following antibodies were used: anti-B220, CD19, IgM^a, CD79B, Qdot 605–streptavidin, and 7AAD. HyHEL9 antibody conjugated to Alex Fluor 647 was performed in-house with a monoclonal antibody labeling kit (Molecular Probes). Cells were first stained with 1 $\mu\text{g/ml}$ HEL protein before staining with the

HyHEL9 antibody. FlowJo (Tree Star) software was used to analyze the flow cytometry data.

Western blot analysis

Transduced B cells were cultured without anti-CD40 for 24 h and EGFP⁺ cells sorted using FACSAria I and II (BD) cell sorter and washed twice with cold PBS. For Western blot analysis, cytoplasmic proteins were extracted from 10⁶ cells using the NE-PER protein extraction kit (78833; Thermo Fisher Scientific) per the manufacturer’s protocol. For Endo H treatment, 5 $\times 10^5$ cell equivalents in 9- μl protein lysates were mixed with 1 μl of 10 \times glycoprotein denaturing buffer, heated at 100°C for 10 min, and incubated at 37°C with the addition of 2 μl 10 \times G5 reaction buffer and 1 μl Endo H in a total volume of 20 μl for 1 h (P0702; New England Biolabs, Inc.). At the end of the reaction, 10 μl 3 \times SDS sample buffer (0.2 M Tris-HCl, pH 6.8, 10% wt/vol SDS, 30% vol/vol glycerol, 10% vol/vol β -mercaptoethanol, and bromophenol blue) was added to stop the reaction, and samples were stored at –20°C until use.

Lysates were heated briefly at 100°C, microcentrifuged for 1 min at 13,000 rpm, and resolved on a 15% polyacrylamide gel. Resolved proteins were then transferred onto a polyvinylidene fluoride membrane (Bio-Rad Laboratories). Nonspecific antibody binding to the membrane was blocked with 5% wt/vol skim milk in TBST (10 mM Tris-HCl, pH 7.5, 150 mM NaCl, and 0.1% vol/vol Tween 20) for 30 min at room temperature and then probed overnight at 4°C with antibodies to IgM and CD79B. After primary antibody incubation, the membrane was washed three times with TBST and incubated with HRP-conjugated anti-rabbit IgG secondary antibody for 60 min at room temperature. Membranes were then washed at least five times with TBST before detection using enhanced chemiluminescence detection reagent (PerkinElmer) and developed in a darkroom onto Kodak films. Membranes were reprobed with anti- α/β -tubulin antibodies as loading control.

Microarray and quantitative PCR analysis

For microarray analysis, sorted cells were resuspended in TRIzol. Phase separation was performed by the addition of chloroform and centrifugation at 12,000 g for 15 min, followed by isopropanol RNA precipitation. The air-dried RNA pellet was dissolved in RNase-free water, and mRNA expression was analyzed on Affymetrix mouse ST 1.0 arrays as per the manufacturer’s instructions. Microarray data were subjected to quality control, normalization, and differential expression analysis in limma (Ritchie et al., 2015). Quality control reviewed reconstructed array images, distribution of probe intensities, M(log ratio) versus A(mean average) plots, fitting of a probe level model in the oligo package (Carvalho and Irizarry, 2010) to generate box plots of relative log expression and normalized unscaled standard errors. One of three independent samples of sorted cells in each experimental group was excluded on the basis of insufficient quality. The final set of eight sam-

ples was normalized using PLM (Carvalho and Irizarry, 2010) and resulting probe weights were used to derive weights for transcript expression estimates on each array suitable for use with limma in a linear model, comparing gene expression in MYD88^{L265P} cells with each of the other groups. CAMERA (Wu and Smyth, 2012) was used to query for enrichment of differentially expressed genes against predefined sets of hallmark, curated, and immunological signature gene sets defined in MSigDB (Subramanian et al., 2005). Microarray data that support the findings of this study have been deposited in Gene Expression Omnibus (accession no. GSE99775).

For quantitative RT-PCR, total RNA was extracted from sorted EGFP⁺ cells with TRIzol (Thermo Fisher Scientific). For each sample, an equal amount of total RNA was reverse-transcribed to cDNA with SuperScript II reverse transcription (Invitrogen) for 2 h at 42°C. Dilution (1:100) of the cDNA stock was used to set up TaqMan quantitative RT-PCR on an ABI7500 instrument (Applied Biosystems) using the following mouse TaqMan probes (Thermo Fisher Scientific): *Myd88* (Mm00440338_m1), *Cd79a* (Mm00432423_m1), *Cd79b*, (Mm00434143_m1), and *Ighm* (Mm01718955_g1). Data were normalized to β -actin expression: ACTB-F, 5'-GCCTTCCTTCTTGGGTATGGAA-3', ACTB-R, 5'-GGCGGACTGTTACTGAGCTG-3'.

Statistical analysis

Data were generated and analyzed using Prism version 5.0 (GraphPad Software). Statistically significant p-values of <0.05, <0.01, and <0.001, determined by two-tailed unpaired Student's *t* test or ANOVA, are indicated where applicable.

Online supplemental material

Fig. S1 shows open reading frames inserted into *Cd79b* 5' UTRs. Fig. S2 shows CD138 expression on EGFP⁺ cells transduced with the indicated vector and analyzed 11 d after adoptive transfer into Rag1^{-/-} recipient mice. Table S1 shows gene set enrichment analysis of MYD88^{L265P}- versus CARD11^{L232LI}-expressing B cells. Table S2 shows hallmark gene sets enriched in MYD88^{L265P}- versus CARD11^{L232LI}-expressing B cells. Table S3 shows curated gene sets enriched in MYD88^{L265P}- versus CARD11^{L232LI}-expressing B cells. Table S4 shows a complete microarray dataset comparing B cells expressing MYD88^{L265P} with cells expressing empty vector, CARD11^{L232LI}, or IKKB^{K171E}. Tables S1–S4 are provided as Excel files.

ACKNOWLEDGMENTS

We thank the Australian Phenomics Facility for expert care and genotyping of animals, the Australian Cancer Research Foundation Biomolecular Resource Facility for sequencing and microarray, and the John Curtin School of Medical Research image and cytometry facility for cell sorting.

J.Q. Wang was supported by an Australian Postgraduate Award and an Australian National University Postgraduate Scholarship. H.M. Yoo was supported by a Korean Visiting Scientist Training Award Fellowship from the Korea Health Industry Development Institute (HI15C1075). C.C. Goodnow was supported by National Health

and Medical Research Council (NHMRC) Australia Fellowship 585490 and NHMRC Senior Principal Research Fellowship 1081858. The research was supported by NHMRC grants to C.C. Goodnow (1016953 and 1113904) and to K. Horikawa (1086770).

The authors declare no competing financial interests.

Author contributions: J.Q. Wang designed and performed experiments, analyzed data, and drafted the manuscript. Y.S. Jeelall, E.L. Batchelor, and S.M. Kaya assisted with experiments. P. Humburg analyzed the microarray data. H.M. Yoo performed and analyzed the quantitative PCR experiments. K. Horikawa conceived the study and constructed the vectors. C.C. Goodnow and K. Horikawa initiated, designed, supervised, and interpreted the experiments and revised the manuscript.

Submitted: 1 September 2016

Revised: 30 April 2017

Accepted: 13 June 2017

REFERENCES

- Akira, S., and K. Takeda. 2004. Toll-like receptor signalling. *Nat. Rev. Immunol.* 4:499–511. <http://dx.doi.org/10.1038/nri1391>
- Avbelj, M., O.O. Wolz, O. Fekonja, M. Benčina, M. Repič, J. Mavri, J. Krüger, C. Schärfe, M. Delmiro Garcia, G. Panter, et al. 2014. Activation of lymphoma-associated MyD88 mutations via allosteric-induced TIR-domain oligomerization. *Blood.* 124:3896–3904. <http://dx.doi.org/10.1182/blood-2014-05-573188>
- Bell, S.E., and C.C. Goodnow. 1994. A selective defect in IgM antigen receptor synthesis and transport causes loss of cell surface IgM expression on tolerant B lymphocytes. *EMBO J.* 13:816–826.
- Bonetti, P., M. Testoni, M. Scandurra, M. Ponzoni, R. Piva, A.A. Mensah, A. Rinaldi, I. Kwee, M.G. Tibiletti, J. Iqbal, et al. 2013. Deregulation of ETS1 and FLI1 contributes to the pathogenesis of diffuse large B-cell lymphoma. *Blood.* 122:2233–2241. <http://dx.doi.org/10.1182/blood-2013-01-475772>
- Bories, J.C., D.M. Willerford, D. Grévin, L. Davidson, A. Camus, P. Martin, D. Stéhelin, and F.W. Alt. 1995. Increased T-cell apoptosis and terminal B-cell differentiation induced by inactivation of the Ets-1 proto-oncogene. *Nature.* 377:635–638. <http://dx.doi.org/10.1038/377635a0>
- Calvo, S.E., D.J. Pagliarini, and V.K. Mootha. 2009. Upstream open reading frames cause widespread reduction of protein expression and are polymorphic among humans. *Proc. Natl. Acad. Sci. USA.* 106:7507–7512. <http://dx.doi.org/10.1073/pnas.0810916106>
- Cambier, J.C., C.M. Pleiman, and M.R. Clark. 1994. Signal transduction by the B cell antigen receptor and its coreceptors. *Annu. Rev. Immunol.* 12:457–486. <http://dx.doi.org/10.1146/annurev.iv.12.040194.002325>
- Carvalho, B.S., and R.A. Irizarry. 2010. A framework for oligonucleotide microarray preprocessing. *Bioinformatics.* 26:2363–2367. <http://dx.doi.org/10.1093/bioinformatics/btq431>
- Chan, V.W., F. Meng, P. Soriano, A.L. DeFranco, and C.A. Lowell. 1997. Characterization of the B lymphocyte populations in Lyn-deficient mice and the role of Lyn in signal initiation and down-regulation. *Immunity.* 7:69–81. [http://dx.doi.org/10.1016/S1074-7613\(00\)80511-7](http://dx.doi.org/10.1016/S1074-7613(00)80511-7)
- Cornall, R.J., J.G. Cyster, M.L. Hibbs, A.R. Dunn, K.L. Otipoby, E.A. Clark, and C.C. Goodnow. 1998. Polygenic autoimmune traits: Lyn, CD22, and SHP-1 are limiting elements of a biochemical pathway regulating BCR signaling and selection. *Immunity.* 8:497–508. [http://dx.doi.org/10.1016/S1074-7613\(00\)80554-3](http://dx.doi.org/10.1016/S1074-7613(00)80554-3)
- Cyster, J.G., S.B. Hartley, and C.C. Goodnow. 1994. Competition for follicular niches excludes self-reactive cells from the recirculating B-cell repertoire. *Nature.* 371:389–395. <http://dx.doi.org/10.1038/371389a0>
- Davis, R.E., V.N. Ngo, G. Lenz, P. Tolar, R.M. Young, P.B. Romesser, H. Kohlhammer, L. Lamy, H. Zhao, Y. Yang, et al. 2010. Chronic active B-cell-receptor signalling in diffuse large B-cell lymphoma. *Nature.* 463:88–92. <http://dx.doi.org/10.1038/nature08638>

- Durand, C.A., K. Hartvigsen, L. Fogelstrand, S. Kim, S. Iritani, B. Vanhaesebroeck, J.L. Witzum, K.D. Puri, and M.R. Gold. 2009. Phosphoinositide 3-kinase p110 delta regulates natural antibody production, marginal zone and B-1 B cell function, and autoantibody responses. *J. Immunol.* 183:5673–5684. <http://dx.doi.org/10.4049/jimmunol.0900432>
- Enders, A., P. Bouillet, H. Puthalakath, Y. Xu, D.M. Tarlinton, and A. Strasser. 2003. Loss of the pro-apoptotic BH3-only Bcl-2 family member Bim inhibits BCR stimulation-induced apoptosis and deletion of autoreactive B cells. *J. Exp. Med.* 198:1119–1126. <http://dx.doi.org/10.1084/jem.20030411>
- Gazumyan, A., A. Reichlin, and M.C. Nussenzweig. 2006. Ig beta tyrosine residues contribute to the control of B cell receptor signaling by regulating receptor internalization. *J. Exp. Med.* 203:1785–1794. <http://dx.doi.org/10.1084/jem.20060221>
- Gerondakis, S., and U. Siebenlist. 2010. Roles of the NF-kappaB pathway in lymphocyte development and function. *Cold Spring Harb. Perspect. Biol.* 2:a000182. <http://dx.doi.org/10.1101/cshperspect.a000182>
- Glynn, R., G. Ghandour, J. Rayner, D.H. Mack, and C.C. Goodnow. 2000. B-lymphocyte quiescence, tolerance and activation as viewed by global gene expression profiling on microarrays. *Immunol. Rev.* 176:216–246. <http://dx.doi.org/10.1034/j.1600-065X.2000.00614.x>
- Goodnow, C.C. 2007. Multistep pathogenesis of autoimmune disease. *Cell.* 130:25–35. <http://dx.doi.org/10.1016/j.cell.2007.06.033>
- Goodnow, C.C.J., J. Crosbie, S. Adelstein, T.B. Lavoie, S.J. Smith-Gill, R.A. Brink, H. Pritchard-Briscoe, J.S. Wotherspoon, R.H. Loblay, K. Raphael, et al. 1988. Altered immunoglobulin expression and functional silencing of self-reactive B lymphocytes in transgenic mice. *Nature.* 334:676–682. <http://dx.doi.org/10.1038/334676a0>
- Grillot-Courvalin, C., J.C. Brouet, F. Piller, L.Z. Rassenti, S. Labaume, G.J. Silverman, L. Silberstein, and T.J. Kipps. 1992. An anti-B cell autoantibody from Wiskott-Aldrich syndrome which recognizes i blood group specificity on normal human B cells. *Eur. J. Immunol.* 22:1781–1788. <http://dx.doi.org/10.1002/eji.1830220717>
- Gross, A.J., J.R. Lyandres, A.K. Panigrahi, E.T. Prak, and A.L. DeFranco. 2009. Developmental acquisition of the Lyn-CD22-SHP-1 inhibitory pathway promotes B cell tolerance. *J. Immunol.* 182:5382–5392. <http://dx.doi.org/10.4049/jimmunol.0803941>
- Hayden, M.S., and S. Ghosh. 2012. NF-κB, the first quarter-century: remarkable progress and outstanding questions. *Genes Dev.* 26:203–234. <http://dx.doi.org/10.1101/gad.183434.111>
- Healy, J.I., R.E. Dolmetsch, L.A. Timmerman, J.G. Cyster, M.L. Thomas, G.R. Crabtree, R.S. Lewis, and C.C. Goodnow. 1997. Different nuclear signals are activated by the B cell receptor during positive versus negative signaling. *Immunity.* 6:419–428. [http://dx.doi.org/10.1016/S1074-7613\(00\)80285-X](http://dx.doi.org/10.1016/S1074-7613(00)80285-X)
- Hollenhorst, P.C., L.P. McIntosh, and B.J. Graves. 2011. Genomic and biochemical insights into the specificity of ETS transcription factors. *Annu. Rev. Biochem.* 80:437–471. <http://dx.doi.org/10.1146/annurev.biochem.79.081507.103945>
- Hsu, F.J., and R. Levy. 1995. Preferential use of the VH4 Ig gene family by diffuse large-cell lymphoma. *Blood.* 86:3072–3082.
- Hunter, Z.R., L. Xu, G. Yang, Y. Zhou, X. Liu, Y. Cao, R.J. Manning, C. Tripas, C.J. Patterson, P. Sheehy, and S.P. Treon. 2014. The genomic landscape of Waldenström macroglobulinemia is characterized by highly recurring MYD88 and WHIM-like CXCR4 mutations, and small somatic deletions associated with B-cell lymphomagenesis. *Blood.* 123:1637–1646. <http://dx.doi.org/10.1182/blood-2013-09-525808>
- Jeelall, Y.S., J.Q. Wang, H.D. Law, H. Domasch, H.K. Fung, A. Kallies, S.L. Nutt, C.C. Goodnow, and K. Horikawa. 2012. Human lymphoma mutations reveal CARD11 as the switch between self-antigen-induced B cell death or proliferation and autoantibody production. *J. Exp. Med.* 209:1907–1917. <http://dx.doi.org/10.1084/jem.20112744>
- Kitamura, T., Y. Koshino, F. Shibata, T. Oki, H. Nakajima, T. Nosaka, and H. Kumagai. 2003. Retrovirus-mediated gene transfer and expression cloning: powerful tools in functional genomics. *Exp. Hematol.* 31:1007–1014. [http://dx.doi.org/10.1016/S0301-472X\(03\)00260-1](http://dx.doi.org/10.1016/S0301-472X(03)00260-1)
- Knittel, G., P. Liedgens, D. Korovkina, J.M. Seeger, Y. Al-Baldawi, M. Al-Maarri, C. Fritz, K. Vlantis, S. Bezhanova, A.H. Scheel, et al. German International Cancer Genome Consortium Molecular Mechanisms in Malignant Lymphoma by Sequencing Project Consortium. 2016. B-cell-specific conditional expression of Myd88p.L252P leads to the development of diffuse large B-cell lymphoma in mice. *Blood.* 127:2732–2741. <http://dx.doi.org/10.1182/blood-2015-11-684183>
- Lam, K.P., R. Kühn, and K. Rajewsky. 1997. In vivo ablation of surface immunoglobulin on mature B cells by inducible gene targeting results in rapid cell death. *Cell.* 90:1073–1083. [http://dx.doi.org/10.1016/S0092-8674\(00\)80373-6](http://dx.doi.org/10.1016/S0092-8674(00)80373-6)
- Lamagna, C., P. Scapini, J.A. van Ziffle, A.L. DeFranco, and C.A. Lowell. 2013. Hyperactivated MyD88 signaling in dendritic cells, through specific deletion of Lyn kinase, causes severe autoimmunity and inflammation. *Proc. Natl. Acad. Sci. USA.* 110:E3311–E3320. <http://dx.doi.org/10.1073/pnas.1300617110>
- Lamagna, C., Y. Hu, A.L. DeFranco, and C.A. Lowell. 2014. B cell-specific loss of Lyn kinase leads to autoimmunity. *J. Immunol.* 192:919–928. <http://dx.doi.org/10.4049/jimmunol.1301979>
- Lenz, G., and L.M. Staudt. 2010. Aggressive lymphomas. *N. Engl. J. Med.* 362:1417–1429. <http://dx.doi.org/10.1056/NEJMra0807082>
- Lenz, G., R.E. Davis, V.N. Ngo, L. Lam, T.C. George, G.W. Wright, S.S. Dave, H. Zhao, W. Xu, A. Rosenwald, et al. 2008. Oncogenic CARD11 mutations in human diffuse large B cell lymphoma. *Science.* 319:1676–1679. <http://dx.doi.org/10.1126/science.1153629>
- Lin, S.C., Y.C. Lo, and H. Wu. 2010. Helical assembly in the MyD88-IRAK4-IRAK2 complex in TLR/IL-1R signalling. *Nature.* 465:885–890. <http://dx.doi.org/10.1038/nature09121>
- Lohr, J.G., P. Stojanov, S.L. Carter, P. Cruz-Gordillo, M.S. Lawrence, D. Auclair, C. Sougne, B. Knoechel, J. Gould, G. Saksena, et al. Multiple Myeloma Research Consortium. 2014. Widespread genetic heterogeneity in multiple myeloma: implications for targeted therapy. *Cancer Cell.* 25:91–101. <http://dx.doi.org/10.1016/j.ccr.2013.12.015>
- Lossos, I.S., C.Y. Okada, R. Tibshirani, R. Warnke, J.M. Vose, T.C. Greiner, and R. Levy. 2000. Molecular analysis of immunoglobulin genes in diffuse large B-cell lymphomas. *Blood.* 95:1797–1803.
- Luo, W., J. Mayeux, T. Gutierrez, L. Russell, A. Getahun, J. Müller, T. Tedder, J. Parnes, R. Rickert, L. Nitschke, et al. 2014. A balance between B cell receptor and inhibitory receptor signaling controls plasma cell differentiation by maintaining optimal Ets1 levels. *J. Immunol.* 193:909–920. <http://dx.doi.org/10.4049/jimmunol.1400666>
- Mori, S., R.E. Rempel, J.T. Chang, G. Yao, A.S. Lagoo, A. Potti, A. Bild, and J.R. Nevins. 2008. Utilization of pathway signatures to reveal distinct types of B lymphoma in the Emicro-myc model and human diffuse large B-cell lymphoma. *Cancer Res.* 68:8525–8534. <http://dx.doi.org/10.1158/0008-5472.CAN-08-1329>
- Ngo, V.N., R.M. Young, R. Schmitz, S. Jhavar, W. Xiao, K.H. Lim, H. Kohlhammer, W. Xu, Y. Yang, H. Zhao, et al. 2011. Oncogenically active MYD88 mutations in human lymphoma. *Nature.* 470:115–119. <http://dx.doi.org/10.1038/nature09671>
- Nutt, S.L., A.M. Morrison, P. Dörfler, A. Rolink, and M. Busslinger. 1998. Identification of BSAP (Pax-5) target genes in early B-cell development by loss- and gain-of-function experiments. *EMBO J.* 17:2319–2333. <http://dx.doi.org/10.1093/emboj/17.8.2319>
- Ottensmeier, C.H., A.R. Thompssett, D. Zhu, B.S. Wilkins, J.W. Sweetenham, and F.K. Stevenson. 1998. Analysis of VH genes in follicular and diffuse lymphoma shows ongoing somatic mutation and multiple isotype transcripts in early disease with changes during disease progression. *Blood.* 91:4292–4299.

- Pascual, V., K. Victor, D. Lelsz, M.B. Spellerberg, T.J. Hamblin, K.M. Thompson, I. Randen, J. Natvig, J.D. Capra, and F.K. Stevenson. 1991. Nucleotide sequence analysis of the V regions of two IgM cold agglutinins. Evidence that the VH4-21 gene segment is responsible for the major cross-reactive idiotype. *J. Immunol.* 146:4385–4391.
- Pasqualucci, L., M. Compagno, J. Houldsworth, S. Monti, A. Grunn, S.V. Nandula, J.C. Aster, V.V. Murty, M.A. Shipp, and R. Dalla-Favera. 2006. Inactivation of the PRDM1/BLIMP1 gene in diffuse large B cell lymphoma. *J. Exp. Med.* 203:311–317. <http://dx.doi.org/10.1084/jem.20052204>
- Poullain, S., C. Roumier, S. Galiègue-Zouitina, A. Daudignon, C. Herbaux, R. Aijjou, A. Lainelle, N. Broucqsaault, E. Bertrand, S. Manier, et al. 2013. Genome wide SNP array identified multiple mechanisms of genetic changes in Waldenström macroglobulinemia. *Am. J. Hematol.* 88:948–954. <http://dx.doi.org/10.1002/ajh.23545>
- Puente, X.S., M. Pinyol, V. Quesada, L. Conde, G.R. Ordóñez, N. Villamor, G. Escaramis, P. Jares, S. Beà, M. González-Díaz, et al. 2011. Whole-genome sequencing identifies recurrent mutations in chronic lymphocytic leukaemia. *Nature.* 475:101–105. <http://dx.doi.org/10.1038/nature10113>
- Pugh-Bernard, A.E., G.J. Silverman, A.J. Cappione, M.E. Villano, D.H. Ryan, R.A. Insel, and I. Sanz. 2001. Regulation of inherently autoreactive VH4-34 B cells in the maintenance of human B cell tolerance. *J. Clin. Invest.* 108:1061–1070. <http://dx.doi.org/10.1172/JCI200112462>
- Reed, J.H., J. Jackson, D. Christ, and C.C. Goodnow. 2016. Clonal redemption of autoantibodies by somatic hypermutation away from self-reactivity during human immunization. *J. Exp. Med.* 213:1255–1265. <http://dx.doi.org/10.1084/jem.20151978>
- Reth, M., and J. Wienands. 1997. Initiation and processing of signals from the B cell antigen receptor. *Annu. Rev. Immunol.* 15:453–479. <http://dx.doi.org/10.1146/annurev.immunol.15.1.453>
- Ritchie, M.E., B. Phipson, D. Wu, Y. Hu, C.W. Law, W. Shi, and G.K. Smyth. 2015. limma powers differential expression analyses for RNA-sequencing and microarray studies. *Nucleic Acids Res.* 43:e47. <http://dx.doi.org/10.1093/nar/gkv007>
- Rui, L., C.G. Vinuesa, J. Blasioli, and C.C. Goodnow. 2003. Resistance to CpG DNA-induced autoimmunity through tolerogenic B cell antigen receptor ERK signaling. *Nat. Immunol.* 4:594–600. <http://dx.doi.org/10.1038/ni924>
- Rui, L., J.I. Healy, J. Blasioli, and C.C. Goodnow. 2006. ERK signaling is a molecular switch integrating opposing inputs from B cell receptor and T cell cytokines to control TLR4-driven plasma cell differentiation. *J. Immunol.* 177:5337–5346. <http://dx.doi.org/10.4049/jimmunol.177.8.5337>
- Rui, L., R. Schmitz, M. Ceribelli, and L.M. Staudt. 2011. Malignant pirates of the immune system. *Nat. Immunol.* 12:933–940. <http://dx.doi.org/10.1038/ni.2094>
- Silberstein, L.E., L.C. Jefferies, J. Goldman, D. Friedman, J.S. Moore, P.C. Nowell, D. Roelcke, W. Pruzanski, J. Roudier, and G.J. Silverman. 1991. Variable region gene analysis of pathologic human autoantibodies to the related i and I red blood cell antigens. *Blood.* 78:2372–2386.
- Srinivasan, L., Y. Sasaki, D.P. Calado, B. Zhang, J.H. Paik, R.A. DePinho, J.L. Kutok, J.F. Kearney, K.L. Otipoby, and K. Rajewsky. 2009. PI3 kinase signals BCR-dependent mature B cell survival. *Cell.* 139:573–586. <http://dx.doi.org/10.1016/j.cell.2009.08.041>
- Subramanian, A., P. Tamayo, V.K. Mootha, S. Mukherjee, B.L. Ebert, M.A. Gillette, A. Paulovich, S.L. Pomeroy, T.R. Golub, E.S. Lander, and J.P. Mesirov. 2005. Gene set enrichment analysis: a knowledge-based approach for interpreting genome-wide expression profiles. *Proc. Natl. Acad. Sci. USA.* 102:15545–15550. <http://dx.doi.org/10.1073/pnas.0506580102>
- Swift, S., J. Lorens, P. Achacoso, and G.P. Nolan. 2001. Rapid production of retroviruses for efficient gene delivery to mammalian cells using 293T cell-based systems. *Curr. Protoc. Immunol.* Chapter 10:Unit 10.17C.
- Thome, M. 2004. CARMA1, BCL-10 and MALT1 in lymphocyte development and activation. *Nat. Rev. Immunol.* 4:348–359. <http://dx.doi.org/10.1038/nri1352>
- Treon, S.P., L. Xu, G. Yang, Y. Zhou, X. Liu, Y. Cao, P. Sheehy, R.J. Manning, C.J. Patterson, C. Tripsas, et al. 2012. MYD88 L265P somatic mutation in Waldenström's macroglobulinemia. *N. Engl. J. Med.* 367:826–833. <http://dx.doi.org/10.1056/NEJMoa1200710>
- Verstrepen, L., I. Carpentier, and R. Beyaert. 2014. The biology of A20-binding inhibitors of NF-kappaB activation (ABINs). *Adv. Exp. Med. Biol.* 809:13–31. http://dx.doi.org/10.1007/978-1-4939-0398-6_2
- Vyncke, L., C. Bovijn, E. Pauwels, T. Van Acker, E. Ruysinck, E. Burg, J. Tavernier, and F. Peelman. 2016. Reconstructing the TIR side of the Myddosome: a paradigm for TIR-TIR interactions. *Structure.* 24:437–447. <http://dx.doi.org/10.1016/j.str.2015.12.018>
- Wang, D., S.A. John, J.L. Clements, D.H. Percy, K.P. Barton, and L.A. Garrett-Sinha. 2005. Ets-1 deficiency leads to altered B cell differentiation, hyperresponsiveness to TLR9 and autoimmune disease. *Int. Immunol.* 17:1179–1191. <http://dx.doi.org/10.1093/intimm/dxh295>
- Wang, J.Q., Y.S. Jeelall, B. Beutler, K. Horikawa, and C.C. Goodnow. 2014. Consequences of the recurrent MYD88^{L265P} somatic mutation for B cell tolerance. *J. Exp. Med.* 211:413–426. <http://dx.doi.org/10.1084/jem.20131424>
- Wang, J.Q., B. Beutler, C.C. Goodnow, and K. Horikawa. 2016. Inhibiting TLR9 and other UNC93B1-dependent TLRs paradoxically increases accumulation of MYD88^{L265P} plasmablasts in vivo. *Blood.* 128:1604–1608. <http://dx.doi.org/10.1182/blood-2016-03-708065>
- Wang, L., M.S. Lawrence, Y. Wan, P. Stojanov, C. Sougnez, K. Stevenson, L. Werner, A. Sivachenko, D.S. DeLuca, L. Zhang, et al. 2011. SF3B1 and other novel cancer genes in chronic lymphocytic leukemia. *N. Engl. J. Med.* 365:2497–2506. <http://dx.doi.org/10.1056/NEJMoa1109016>
- Wilson, W.H., R.M. Young, R. Schmitz, Y. Yang, S. Pittaluga, G. Wright, C.J. Lih, P.M. Williams, A.L. Shaffer, J. Gerecitano, et al. 2015. Targeting B cell receptor signaling with ibrutinib in diffuse large B cell lymphoma. *Nat. Med.* 21:922–926. <http://dx.doi.org/10.1038/nm.3884>
- Wu, D., and G.K. Smyth. 2012. Camera: a competitive gene set test accounting for inter-gene correlation. *Nucleic Acids Res.* 40:e133. <http://dx.doi.org/10.1093/nar/gks461>
- Xu, L., Z.R. Hunter, G. Yang, Y. Zhou, Y. Cao, X. Liu, E. Morra, A. Trojani, A. Greco, L. Arcaini, et al. 2013. MYD88 L265P in Waldenström macroglobulinemia, immunoglobulin M monoclonal gammopathy, and other B-cell lymphoproliferative disorders using conventional and quantitative allele-specific polymerase chain reaction. *Blood.* 121:2051–2058. <http://dx.doi.org/10.1182/blood-2012-09-454355>
- Young, R.M., A.L. Shaffer III, J.D. Phelan, and L.M. Staudt. 2015. B-cell receptor signaling in diffuse large B-cell lymphoma. *Semin. Hematol.* 52:77–85. <http://dx.doi.org/10.1053/j.seminhematol.2015.01.008>
- Zhu, D., R.E. Hawkins, T.J. Hamblin, and F.K. Stevenson. 1994. Clonal history of a human follicular lymphoma as revealed in the immunoglobulin variable region genes. *Br. J. Haematol.* 86:505–512. <http://dx.doi.org/10.1111/j.1365-2141.1994.tb04780.x>
- Zikherman, J., R. Parameswaran, and A. Weiss. 2012. Endogenous antigen tunes the responsiveness of naive B cells but not T cells. *Nature.* 489:160–164. <http://dx.doi.org/10.1038/nature11311>